EXPERIMENTATION AND OPTIMIZATION OF A HEAT PUMP INTEGRATED DISHWASHER

A THESIS SUBMITTED TO
THE GRADUATE SCHOOL OF NATURAL AND APPLIED SCIENCES
OF
MIDDLE EAST TECHNICAL UNIVERSITY

BY

ERKAN KÜTÜK

IN PARTIAL FULFILLMENT OF THE REQUIREMENTS
FOR
THE DEGREE OF MASTER OF SCIENCE
IN
MECHANICAL ENGINEERING

AUGUST 2019

Approval of the thesis:

EXPERIMENTATION AND OPTIMIZATION OF A HEAT PUMP INTEGRATED DISHWASHER

submitted by **ERKAN KÜTÜK** in partial fulfillment of the requirements for the degree of **Master of Science in Mechanical Engineering Department, Middle East Technical University** by,

Prof. Dr. Halil Kalıpçılar
Dean, Graduate School of **Natural and Applied Sciences** ________________

Prof. Dr. M. A. Sahir Arıkan
Head of Department, **Mechanical Engineering** ________________

Assist. Prof. Dr. Özgür Bayer
Supervisor, **Mechanical Engineering, METU** ________________

Examining Committee Members:

Prof. Dr. İlker Tarı
Mechanical Engineering Dept., METU ________________

Assist. Prof. Dr. Özgür Bayer
Mechanical Engineering, METU ________________

Prof. Dr. Tuba Okutucu Özyurt
Mechanical Engineering Dept., METU ________________

Assist. Prof. Dr. M. Kemal Tural
Industrial Engineering Dept., METU ________________

Prof. Dr. Murat Köksal
Mechanical Engineering Dept., Hacettepe University ________________

Date: 28.08.2019

I hereby declare that all information in this document has been obtained and presented in accordance with academic rules and ethical conduct. I also declare that, as required by these rules and conduct, I have fully cited and referenced all material and results that are not original to this work.

Name, Surname: Erkan Kütük

Signature:

ABSTRACT

EXPERIMENTATION AND OPTIMIZATION OF A HEAT PUMP INTEGRATED DISHWASHER

Kütük, Erkan
Master of Science, Mechanical Engineering
Supervisor: Assist. Prof. Dr. Özgür Bayer

August 2019, 89 pages

This study aims to develop the optimization of heat pump system working parameters for minimum energy consumption, operating time and noise level for a novel dishwasher. In an integrated heat pump system, compressor speed (N) and air flow rate ($\dot{V}$) over the evaporator are selected as variables that affects energy consumption (E), acoustic level (A) and operating time (t). Due to the international energy regulations for household appliances, energy efficiency is highly important and for user comfort, operation time and noise level are critical. In order to perform optimization, experiments have been conducted with various parameters and outputs are recorded. Since, it is impossible to test all range of selected parameters and their combinations, experiments are conducted with pre-defined parameters which are compressor speeds and air flow rates. In order to estimate all range of parameter value outputs curve fit polynomials are obtained by using experimental data. The experiment results are compared with the results of analytical analysis.

For optimization; energy consumption, operating time and noise level are defined as objective functions. Multi Objective Particle Swarm Optimization (MOPSO) method is used to minimize the objective functions. Optimization is achieved by using Matlab commercial software.

The advantage of heat pump system integration is 302 Wh decrease in energy consumption. However, the main disadvantage is an increase in noise level. Noise level may increase up to 46.8 dBA due to compressor and fan. Heating time is longer with heat pump integrated dishwasher (HPIDW) system with respect to electric resistance dishwasher (ERDW). However, cleaning program algorithm can be changed in order to eliminate this elongation of heating time.

Keywords: Heat Pump, Particle Swarm Optimization, Dishwasher, Compressor, Fan

ÖZ

ISI POMPASI ENTEGRE EDİLMİŞ BULAŞIK MAKİNASI DENEYLERİ VE OPTİMİZASYONU

Kütük, Erkan
Yüksek Lisans, Makina Mühendisliği
Tez Danışmanı: Dr. Öğr. Üyesi Özgür Bayer

Ağustos 2019, 89 sayfa

Bu çalışma, ev cihazının minimum enerji tüketimi, çalışma süresi ve ses seviyesi için ısı pompası çalışma parametrelerinin optimizasyonunu geliştirmeyi hedeflemektedir. Isı pompası sisteminde, enerji tüketimini (E), akustik seviyeyi (A) ve program süresini (t) etkileyen değiştirilebilir parametreler olarak kompresör devri (N) ve buharlaştırıcıdaki hava akış hızı ($\dot{V}$) seçilmiştir. Uluslararası standartlar sebebiyle ev cihazlarında enerji verimliliği oldukça önem arz etmektedir. Kullanıcı konforu için ise program süresi ve ses seviyesi önem taşımaktadır. Parametreler değiştirilerek testler yapılmış ve sonuçlar optimize edilmiştir. Seçilen parametrelerin hepsini test etmek mümkün değildir. Bu nedenle kompresör devri ve hava akış hızları önceden tanımlanarak değişkenler seçilmiş ve testler yapılmıştır. Test edilemeyen çalışma noktalarının sonuçlarını belirleyebilmek için deney verileri kullanılarak en iyi uyum doğruları çizilmiştir. Test sonuçları, analitik hesaplamalar ile karşılaştırılmıştır.

Optimizasyon için enerji tüketimi, program süresi ve ses seviyesi amaç fonksiyonları olarak seçilmiştir. Fonksiyonların minimumunu hesaplamak için Çoklu Amaç Parçacık Sürü Optimizasyonu metodu kullanılmıştır. Optimizasyon Matlab programı kullanılarak gerçekleştirilmiştir.

Enerji tüketiminde 302 Wh azaltma sağlanması ısı pompası entegrasyonunun avantajıdır. Ana dezavantajı ise ses seviyesindeki yükselmedir. Ses seviyesi, kompresör ve fan sebebiyle 46.8 dBA'e kadar artış gösterebilmektedir. Isı pompalı sistemde ısıtma süresi rezistans ısıtıcılı sisteme göre daha uzundur. Ancak, yıkama algoritmasında değişiklik yapılarak süre uzaması elimine edilebilmektedir.

Anahtar Kelimeler: Isı Pompası, Parçacık Sürü Optimizasyonu, Bulaşık Makinası, Kompresör, Fan

To My Family

ACKNOWLEDGEMENTS

Firstly, I would like to express my profound gratitude to Assist. Prof. Dr. Özgür Bayer for his contributions, guidance, and encouragement throughout my graduate studies. It is an honor to be his student.

I would also like to specially thank my colleagues N. Efe Aras, Ufuk Aşkın, Didem Polat, Hasret G. Külahcı, Dilan Güzel, Onur Poyraz, Hüseyin Çalışkan and Dr. Songül Bayraktar for unfailing support.

Lastly, I would like to thank my family for their great support, understanding and encouragement.

TABLE OF CONTENTS

LIST OF TABLES

TABLES

LIST OF FIGURES

FIGURES

LIST OF ABBREVIATIONS

A	Noise Level
AC	Alternating Current, Air Conditioner
ACO	Ant Colony Algorithm
ASHPWH	Air Source Heat Pump Water Heater
C	Clearance Factor, Constant
Cat.	Category
CCPSO	Constriction Coefficient Particle Swarm Optimization
CENELEC	European Committee for Electrotechnical Standardization
CFC	Chlorofluorocarbon
CMOPSO	Constrained Multi Objective Particle Swarm Optimization
COP	Coefficient of Performance
Cp	Constant Pressure Specific Heat
D	Bore Diameter
DAS	Data Acquisition System
DC	Direct Current
Dist.	Distribution
DW	Dishwasher
E	Energy Consumption
EA	Evolutionary Algorithm
EC	Evolutionary Computation

EEV	Electronic Expansion Valve
EN	European Standard
EPDM	Ethylene Propylene Diene Monomers
ERDW	Electric Resistance Dishwasher
f	Friction Factor, Fraction
GA	Genetic Algorithm
GWP	Global Warming Potential
h	Specific Enthalpy
HCFC	Hydrochlorofluorocarbon
HPIDW	Heat Pump Integrated Dishwasher
IEC	International Electrotechnical Commission
IPSO	Improved Particle Swarm Optimization
ISO	International Organization of Standardization
L	Stroke
LMTD	Log Mean Temperature Difference
m	Mass, Re-expansion Index
MA	Memetic Algorithm
MOPSO	Multi Objective Particle Swarm Optimization
N	Compressor Speed
n	Compression Index
NTU	Number of Transfer Units
ODP	Ozone Depletion Potential

P	Pressure
PSO	Particle Swarm Optimization
$\dot{Q}$	Heat Transfer Rate
Qty.	Quantity
RH	Relative Humidity
SFL	Shuffled Frog Algorithm
SWM	Support Vector Machine
t	Operating Time
T	Temperature
TC	Technical Committee
TEWI	Total Equivalent Warming Impact
TFHE	Three Fluid Heat Exchanger
Unc.	Uncertainty
$\dot{V}$	Air Flow Rate
Vp	Swept Volume
$\dot{W}$	Power Supplied by the Compressor

Subscripts

1,2…	States
a,b,c,d	Coefficients of Curve Fit Equations
d,s	Discharge, Suction
l,h	Lower, higher

ps, pd	Pressures Through Suction and Discharge Valves, Respectively
comp	Compressor
cond	Condenser
eva	Evaporator

<u>Greek Symbols</u>

η	Efficiency
η_v	Overall Volumetric Efficiency
ν	Specific Volume
ρ	Density

CHAPTER 1

INTRODUCTION

1.1. General

Nowadays, more energy efficient household appliances become preferable with increasing environmental consciousness. Therefore, improvements in production technologies and new innovative designs make engineers able to produce white goods consuming less resources.

Heat pump system is one of the alternatives to conventional resistance heater. Refrigeration cycles are used in refrigerators for a long time, whereas in the household appliances market, heat pump systems come in sight with their integration to drying machines in recent years and in domestic dishwashers lately.

Many patent applications have been made with various companies that involve heat pumps for heating washing water and drying of dishes.

1.2. Definition

The heat pump system is composed of a compressor, an evaporator, a condenser, a capillary tube, evaporator fans and a drain pump.

Compressor is used for increasing the pressure of the refrigerant and supply pressure difference between evaporator and condenser.

Evaporator is a heat exchanger which transfers heat to the refrigerant from the air flowing over the fins and makes it evaporate.

Condenser, at the exit of which the refrigerant turns into liquid phase, works as a heat exchanger enabling the transfer of heat from the refrigerant to washing water.

Capillary tube is a kind of narrow pipe which provides pressure difference among its ends. It is placed in between the evaporator and the condenser in which refrigerant is at low and high pressures.

Evaporator fans are placed in front of the evaporator and supply air flow in order to increase the heat transfer with forced convection.

Since the evaporator surface temperature is below the dew point temperature of the moist air flowing over it, water condenses on the surface and a mini pump is used to discharge the condensing water to the drain pump.

In the present design, R600a refrigerant is used with reciprocating type compressor. Coil type evaporator and condenser are integrated.

1.3. Motivation

In current design of domestic dishwasher, electrical resistance type heater is used to heat the washing water. The heater consumes high energy during a cleaning program when compared with other components in the machine. Therefore, in order to make energy efficient dishwasher, energy consumption to heat washing water has to be decreased.

In present, heat pump system is integrated into a domestic dishwasher to increase energy efficiency. Heat pump is used for heating the washing water without using resistance heater. However, there is one major restriction that effects the design and performance of heat pump system highly. On the contrary of dryer and refrigerator, the volume for fitting heat pump system is smaller. Therefore, undersized component designs are compulsory.

Coil type evaporator, helical condenser, fans and variable speed compressor are used in the system. However, since the volume of the components are restricted, to obtain higher performance, air flow rate can be increased to make higher heat transfer through evaporator. Increasing air flow rate also increases the noise level. On the other hand, increasing compressor speed also affects energy consumption and noise level. Both decreasing air flow rate and compressor speed also affect the dishwasher operating time. Therefore, an optimization is necessary to maximize energy efficiency while minimizing noise level and operating time.

In this thesis study, experiment with ERDW and novel HPIDW have been performed with various compressor speed and air flow rates. Energy consumption, noise level and operating time were recorded with changing these parameters. With the results, optimization has been achieved for a better energy efficient machine.

CHAPTER 2

LITERATURE REVIEW INCLUDING ENERGY STANDARDS

2.1. Literature Survey

The detailed literature survey on heat pump system studies has been done. In brief, investigation of heat pump system usability on dishwasher has not been studied extensively yet. Mainly, some experiments are conducted, and models are tested for domestic dryers, air conditioners, refrigerators and air conditioner systems in cars. In the dishwasher, the heat pump systems have different working conditions since the aim is to heat the washing water. The evaporation and condensation temperatures are higher. Also, for dishwashers there is a space limitation for heat exchangers. In the literature, there is not enough information for these kinds of applications. When compared with resistance heater, heat pump application for water heating on the household appliances seems highly advantageous in terms of energy efficiency. After heating, air conditioning, and lighting; water heating has the fourth largest energy consumption item in the commercial buildings including extensive laundry or dishwashing [1].

The importance of energy consumption does not only come from the consumer but also from environmental concerns. Since greenhouse gases resulting from human consumption of oil, gas and coal are the main cause of global warming, energy efficient buildings are encouraged by government policies. As a result, production of heat pump systems for different applications is increasing [2].

2.1.1. Heat Pump Applications

Bengtsson et al. [3] studied the heat pump system for domestic dishwasher. Experimental setup and simulation model improvement of a HPIDW was stated by Bengtsson. Energy consumption was researched by varying the cylinder volume of compressor and the operating time in a transient simulation model. The results of the study show that;

- A HPIDW has 24% less energy consumption compared to a standard domestic dishwasher, with the same operating time and temperatures in the washing and rinsing steps.
- A longer operating time of heat pump system (up to 50 minutes) yields in reduced overall energy consumption.
- Compressor cylinder volume has less effect on overall energy consumption when the operating time of the compressor is more than 60 min.

The study [3] also compared the cleaning cycle for conventional dishwasher and heat pump integrated dishwasher. The temperature during cleaning cycle is given in Figure 2.1. Tap water is taken to the dishwasher in prewash step firstly. In washing and rinsing steps, water is heated. In each step, the washing water is discharged and tap water is entered to the dishwasher.

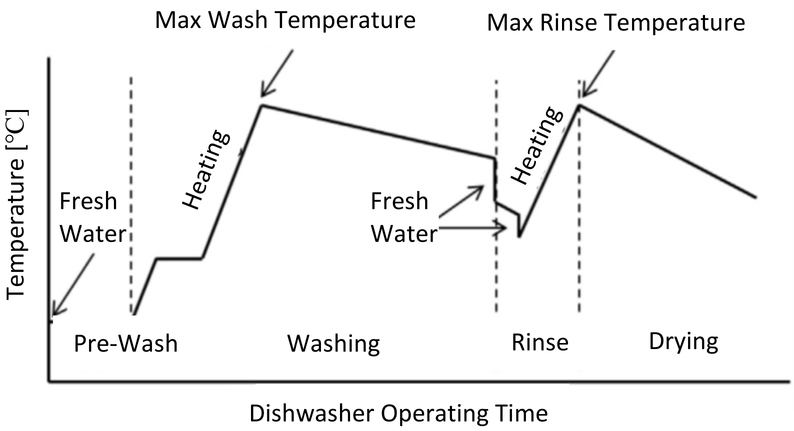

Figure 2.1. Temperature change of washing water during one cleaning cycle [3]

Temperature change of the washing water and the energy storage unit in the transient simulation model is given in Figure 2.2. Temperatures of washing water T_{dw} and the energy storage T_{es} are illustrated. Most of the energy is consumed when the heat pump system and the resistance heater is working.

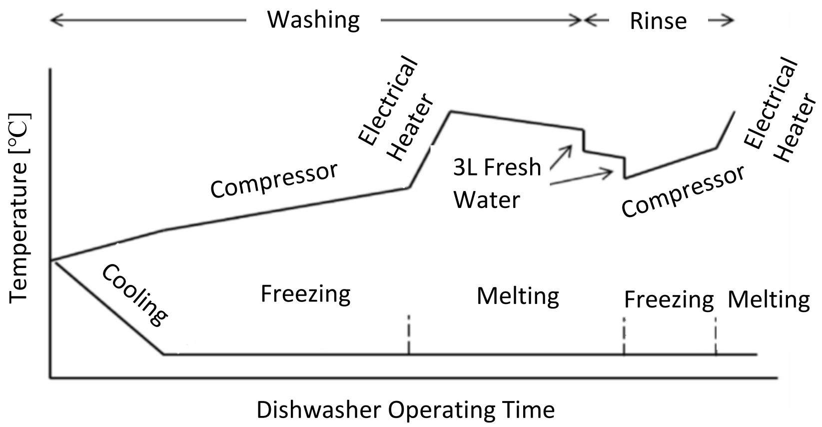

Figure 2.2. Temperature change of the washing water and the energy storage unit in the simulation model [3]

Fardoun et al. [4] tried to predict the performance of a simple air source heat pump water heater (ASHPWH). Heat exchangers in the simulation were designed by using both LMTD and ε-NTU methods and actuator components were modeled by static designs. The model was coded into MATLAB software and used to predict system parameters of interest such as hot water temperature, evaporating and condensing pressures, heat rejected in the condenser, electric power input, heating seasonal performance factor, and coefficient of performance. The results showed that in ASHPWH, energy consumption is reduced about 70% when compared to conventional electrical water heaters.

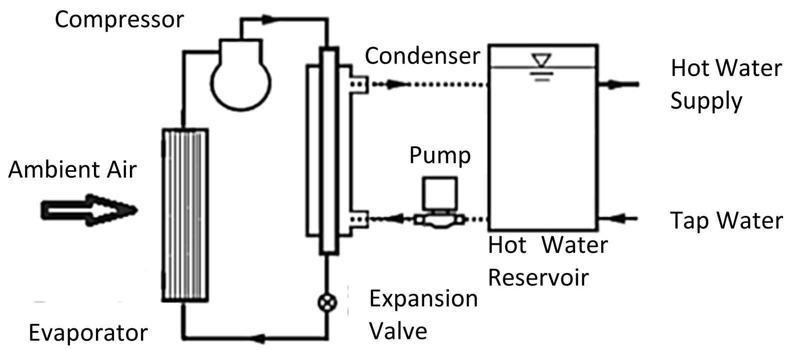

Figure 2.3. Air source water heater [4]

Zhang et al. [5] developed a simulation model of a fin-tube three-fluid heat exchanger with distributed parameter method and validated the model results with experimental data. The performance of different geometric structures and working conditions were investigated. It has generalized that circuit arrangement type has important effect on the performance of fin-tube three-fluid heat exchanger. The heat transfer rate increases with increasing inner tube diameter and it is fixed at 6.0 mm considering manufacture. The heat transfer rates of the three fluids all increase with increasing flow rate of the hot fluid. Increasing inlet pressure of the hot fluid will improve the heat transfer rates of all the three fluids. With increasing inlet temperature of cold fluid 2 (air), the heat transfer rate of the hot fluid and airside decreases while the heat transfer rate of the other side increases.

Monapatra et al. [6] carried out an experimental study to investigate the performance of a three fluid heat exchanger (TFHE). Experimental and analytical temperature distribution data were determined and compared with each other for three fluids along the non-dimensional axial distance of TFHE. The effect of variation in volume flow rate on performance of the TFHE was obtained. The results show that, by increasing the volumetric flow rate of hot water, normal water and air in the TFHE successively, overall heat transfer coefficient is increased in each case. However, the heat transfer effectiveness decreased or increased in different cases, because the variation of effectiveness is dependent on the combined effect of residence time, capacity ratio, R and NTU. TFHE provides optimized performance i.e. higher overall heat transfer coefficients and effectiveness, when flow rate of normal water increased in counter flow configuration. TFHE may be used for space heating and water heating simultaneously for domestic and process heating purposes.

Bengtsson et al. [7] performed a parameter study on heat pump integrated domestic dishwasher to examine the lowest total use of electricity for R134a, R290, and R600a with distinct cylinder volumes of the compressor. The outcomes regarding total electricity consumption and the total equivalent warming impact (TEWI) were observed and the compressor cylinder volume was optimized. It is obtained that for the heat pump, a dishwasher's total electricity use is about 25% lower than the electric-element variant, independent of which refrigerant is used, i.e. R134a, R290, or R600a. The suggestion for reducing dishwasher's complete global warming impact is to focus on replacing all standard dishwasher with heat pump dishwasher using a low-GWP refrigerant such as R290 or R600a.

Bengtsson et al. [8] conducted a conceptual study that evaluates a new drying technique in a heat pump dishwasher. Drying efficiency was researched in an experimental set-up by varying airflow parameters, drying time, quantity of ice in the water tank and starting temperature of drying. The following conclusions can be taken on the basis of these outcomes, which are compared to the current drying technique. The new closed drying method is more energy-efficient than an open drying method available on the market since it reduces the usage of energy consumption by 39 Wh. With this drying technique, the amount of ice required for the experimental set-up is 1 kg. The starting temperature and the drying time considerably influence the drying efficiency.

Flück et al. [9] presented a dishwasher with the heat pump cleaning program demonstrating that power consumption can be lowered up to 50%. Other cleaning programs would also be developed with the heat pump in addition to the advantage of using the eco program where only the heat pump is activated. With the parallel use of heat pump and electrical resistance heaters, the complete heating power can be improved resulting to lower operating time. In addition, the power consumption of these programs is also decreased relative to electrical resistance heating.

Bengtsson et al. [10] conducted a study about the use of capillary pipes in a heat pump integrated dishwasher with a transient heating period. The compressor and capillary pipe diameter were characterized by a conventional dishwasher. The energy consumption was evaluated in an experimental setup using five pipe sizes with four varying refrigerant amounts. It is concluded that, in the transient heating cycle, a cheaper single capillary tube could be used as a fixed expansion device without raising the usage of electricity relative to a variable expansion device. The lengths proposed by calculations of the capillary pipe lengths were too short for the transient heating phase in a dishwasher. One explanation is that during the experiments sub-cooling exists, however in the calculations it was ignored.

Flück et al. [11] conducted a study comparing energy consumption of a prototype with the other types of dishwashers. Findings indicate that the use of a heat pump system in an open drying dishwasher could decrease the use of electricity by up to 50% relative to electrical resistance heating dishwasher with closed drying method. The decrease is 37.1% compared to an open adsorption system dishwasher. Compared to structurally similar dishwashers (Adora SL from V-ZUG Ltd.) with electrical resistance heating and open drying, the decrease is 32.9%. Since 2014, a dishwasher has been accessible on the market with a monovalent heat pump system and open drying system.

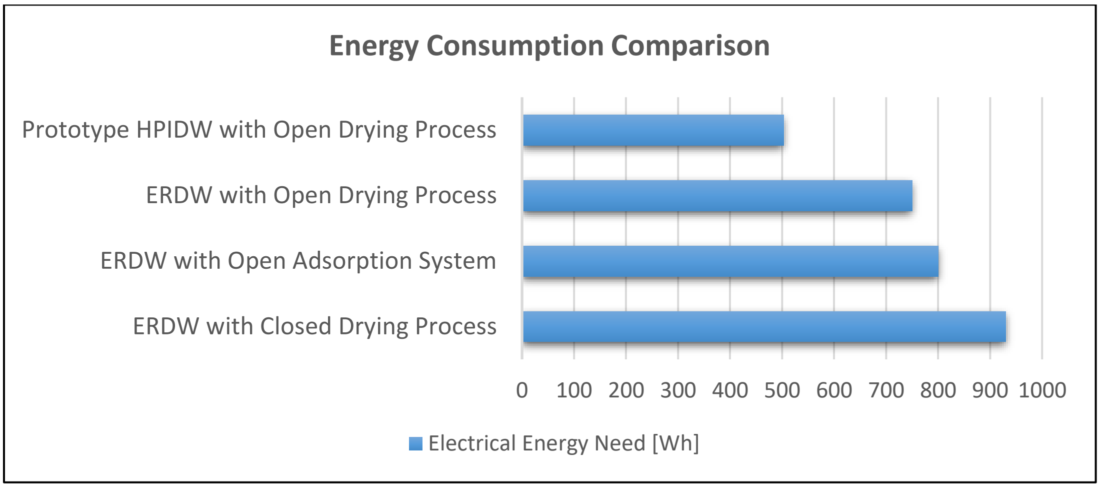

Figure 2.4. Comparison of the electrical energy needs of different dishwashers [11]

Abu-Heiba et al. [12] introduced a lumped capacitance, quasi-steady state numerical model of a new embedded thermal storage dishwasher. The model provides the energy usage and duration of the drying phase for the cleaning and the drying process. Model results were acquired from a simple set of clean cycle assumptions of 4 washing processes of equal duration, each with 3.78 liter of water. The voltage supplied to the thermoelectric heat pump was parametrically varied. Cleaning water is heated up to maximum 47°C, while the thermal storage was cooled below freezing. Hence, greater heat storage and/or some electrical resistance heating may be necessary.

Park et al. [13] conducted a study about improvements in energy efficiency by raising the water temperature in the tub of household appliance during heater-off cycle. It also offers a helpful simulation model for predicting the rise in the tub's water temperature under various conditions. In this research, the slit-fin and round-tube heat exchanger has the maximum energy efficiency of 5.68 % with the nine-inch blade fan and the additional pump.

Peng et al. [14] presented a quasi-steady Air Source Heat Pump Water Heater (ASHPWH) system model that was evaluated by a prototype with scroll compressor running with R134a under various operating circumstances. Further studies have been done with three different expansion devices, namely electronic expansion valve (EEV), capillary tube, and short tube orifice. As a result, EEV remains the highest performance extension device for ASHPWH. Short tube orifice becomes a better option in terms of efficiency and price rather than capillary tube.

2.1.2. Particle Swarm Optimizations Studies

Zhang et. al. [15] introduced a new constrained multi-objective particle swarm optimization (CMOPSO) algorithm relying on an integrated penalty and a normalized non-dominated sorting method. CMOPSO ranks individuals along with the new objective functions obtained from the adaptive penalty technique. The simulation test findings show accurate convergence and diverse distribution of non-dominant solutions on the true Pareto front revealing that suggested algorithm has excellent performance for generational distance and spacing.

Hosseini et al. [16] optimized the truss constructions with MOPSO. Several examples were evaluated to test the accuracy and effectiveness of the technique. The results obtained by the MOPSO technique are more accurate with respect to evolutionary methods.

Chatterjee et al. [17] suggested a novel PSO version using nonlinear inertia weight variety. This nonlinear variation is implemented in order to make coarse tuning during initial iterations. Therefore, better search of the solution space is achieved quickly. Fine tuning has been done in later iterations so that to obtain the optimum solution with high accuracy. The reliability of the suggested PSO algorithm is tested for varying functions and compared with popular PSO and non-PSO algorithms. The correct selection of exponent n is one of the significant variables in the effective execution. After each iteration, n is adaptively determined on the basis of gradual variation in the fitness function value.

Coello et al. [18] studied on extension of PSO to deal with multi-objective problems. The suggested algorithm is comparatively simple to perform and enhances PSO's exploratory capabilities by implementing a mutation operator. The suggested method was validated using the commonly accepted standard methodology. The findings show that the new approach is a feasible option as it has a competitive performance compared to some of the best evolutionary multi-objective algorithms.

Goh et al. [19] reported MOPSO's efficiency and effectiveness needs to be improved due to increasing complexity of recent applications. In this study a competitive and cooperative co-evolutionary approach is adapted for multi-objective particle swarm optimization algorithm. The proposed competitive and cooperative co-evolutionary multi-objective particle swarm optimization algorithm (CCPSO) was validated through comparisons with existing multi-objective algorithms. Simulation results revealed that CCPSO shows competitive performance as compared to the other algorithms.

Jiang et al. [20] introduced a shuffled complex evolution of the particle swarm optimization algorithm named IPSO to enhance PSO efficiency. In IPSO, population is sampled randomly from the viable space and divided into sub-swarms evolving based on PSO. The method could improve survivability by sharing of the data. Three benchmark functions and a case study were conducted in the simulation part using different algorithms. The performance comparisons show that IPSO is preferable to PSO.

Kao et al. [21] suggested combination of genetic algorithm and particle swarm optimization which is named GA-PSO as a novel approach to optimizing multi-objective functions. GA-PSO integrates the concept of evolving particles initially modeled by GA with the concept of self-improvement of PSO, where particles develop themselves based on social relationships and their private cognition. Therefore, GA-PSO incorporates the advantages of both GA and PSO, and it is a simple and effective model to handle various types of continuous optimization problems. Simulated tests to optimize nonlinear multimodal functions demonstrate that GA-PSO is superior to the other methods in the ability to detect the global optimum.

Lin et al. [22] introduced a particle swarm optimization-based approach, which is able to search for the optimal parameter values to support vector machine (SVM) to achieve a subset of beneficial properties. This optimal subset of properties is then implemented in both training and testing to achieve the ideal classification results. Comparison of the outcomes acquired with other methods shows that the PSO+SVM method has introduced a better classification accuracy.

2.2. Energy Standards for Dishwashers

The International Electrotechnical Commission (IEC) is a worldwide organization for standardization comprising all national electrotechnical committees (IEC National Committees). The object of IEC is to promote international co-operation on all questions concerning standardization in the electrical and electronic fields. To this end and in addition to other activities, IEC publishes international standards, technical specifications, technical reports, publicly available specifications and guides. Their preparation is entrusted to technical committees; any IEC National Committee interested in the subject dealt with may participate in this preparatory work. International, governmental and nongovernmental organizations liaising with the IEC also participate in this preparation. IEC collaborates closely with the International Organization for Standardization (ISO) in accordance with conditions determined by agreement between the two organizations.

For European market, dishwashers are designed to satisfy the requirements mentioned in European Standard EN 50242 “Electric dishwashers for household use - Methods for measuring the performance” [23].

European Standard consists of the text of IEC 60436:2004 [24] prepared by SC 59A, electric dishwashers, of IEC TC 59, performance of household electrical appliances, together with all common modifications necessary for application in Europe. These common modifications have been prepared by the Technical Committee CENELEC TC 59X, consumer information related to household electrical appliances.

The object is to state and define the principal performance characteristics of electric dishwashers for household use and to describe the standard methods of measuring these characteristics.

The EN 50242 standard was approved by Comité Européen de Normalisation Electrotechnique - European Committee for Electrotechnical Standardization (CENELEC) whose members are the national electrotechnical committees of Austria, Belgium, Bulgaria, Croatia, Cyprus, the Czech Republic, Denmark, Estonia, Finland, Former Yugoslav Republic of Macedonia, France, Germany, Greece, Hungary, Iceland, Ireland, Italy, Latvia, Lithuania, Luxembourg, Malta, the Netherlands, Norway, Poland, Portugal, Romania, Slovakia, Slovenia, Spain, Sweden, Switzerland, Turkey and the United Kingdom.

Standard methods of measuring the performance characteristics are determined with corresponding clauses. Cleaning performance, drying performance, energy and water consumption, time and airborne acoustical noise measuring methods are defined in Clause 6 to 9 [23].

According to the EN 50242 standard [23] eco cleaning program is used for energy labeling tests. Eco cleaning program is designed to clean normally soiled tableware and is most efficient program in terms of energy consumption and water usage. In eco cleaning program, cleaning and drying are completed usually with lower temperature (about 50 ℃) and longer operating time.

Similar to the studies in literature [3, 7, 8, 9, 10, 11] the experiments in the present study are conducted according to defined test standard in EN 50242 [23]. On the other hand, this thesis study differs from literature in terms of an air source heat pump system application. In literature, water source heat pump systems are experimented. However, the major disadvantage of water source system is ice formation in the tank where evaporator is located. Due to this reason, there has to be a certain buffer time between dishwasher operation to melt ice in the tank. One other difference of the present work from those in literature is integration of heat pump system into limited space without changing dishwasher size. In addition, this thesis study considers optimization of energy consumption, noise level and operating time by implementing MOPSO method which has not been applied academically to a dishwasher problem yet.

CHAPTER 3

SYSTEM DESIGN AND SPECIFICATIONS

3.1. Heat Pump Cycles

3.1.1. Reversed Carnot Cycle

A heat pump cycle is used to transfer heat from a low temperature medium to high temperature medium by applying work. The reversed Carnot cycle [25] is the most efficient (ideal) heat pump cycle operating between reservoirs at temperatures T_L and T_H.

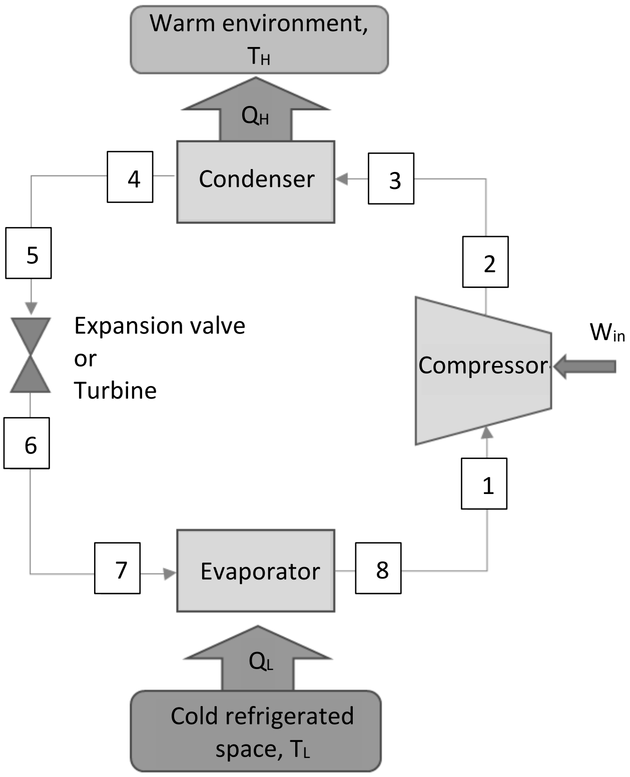

Figure 3.1. Schematic diagram of reversed Carnot and vapor-compression refrigeration cycles [25]

The cycle consists of four processes.

1-2: Isentropic compression of the refrigerant occurs in the compressor by supplying work, W_{in}. This process will increase both its temperature and pressure.

3-4: In the condenser, refrigerant rejects its heat isothermally to high temperature reservoir at T_H with an amount Q_H. So, refrigerant changes its state from saturated vapor to saturated liquid.

5-6: Refrigerant expands adiabatically in the turbine.

7-8: In the evaporator, refrigerant absorbs heat isothermally from a low temperature source at T_L with an amount of Q_L.

In state 2-3, 4-5, 6-7 and 8-1, there are no change occurred.

The reversed Carnot cycle is not a suitable model for actual heat pump cycles since processes 1-2 and 5-6 are not practical. Process 1-2 involves the compression of liquid-vapor mixture, which requires a compressor that will handle two phases, and process 5-6 involves the expansion of high moisture content refrigerant in the turbine.

T-s and P-h diagrams of reversed Carnot cycle are presented in Figure 3.2. and 3.3.

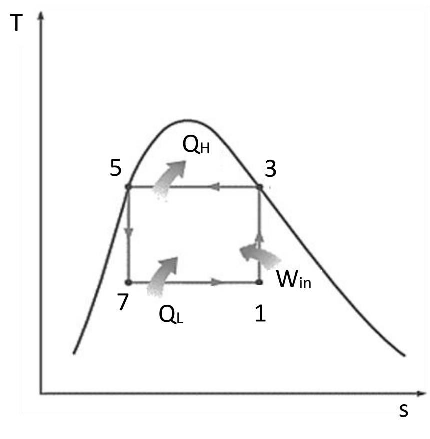

Figure 3.2. T-s Diagram of reversed Carnot cycle [25]

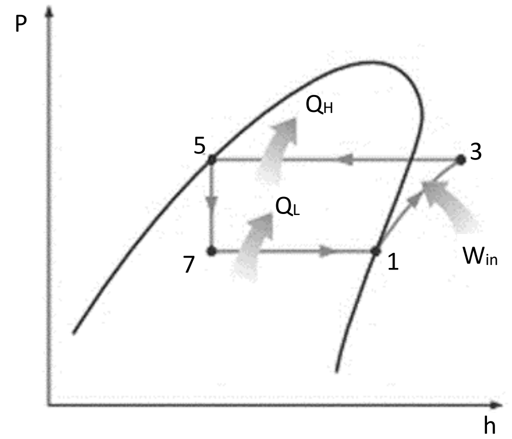

Figure 3.3. P-h Diagram of the reversed Carnot cycle [25]

The performance of a heat pump is evaluated by how much heat transfer Q_H occurs into the warm space compared with how much work input W_{in} is required.

$$(COP)_{Carnot} = \frac{Q_H}{W_{in}} = \frac{Q_H}{Q_H - Q_L} = \frac{1}{1-(T_L/T_H)} \tag{1}$$

COP of the heat pump Carnot cycle increases when T_L rises or T_H falls.

3.1.2. The Ideal and Actual Vapor-Compression Refrigeration Cycles

The ideal vapor compression refrigeration cycle [25] is the ideal model for refrigeration systems, A-C systems and heat pumps. Unlike the reversed Carnot cycle, the refrigerant is vaporized completely before it is compressed, and the turbine is replaced with a throttling device.

Four processes of ideal cycle are;

1- 2: Isentropic compression in a compressor

3- 4: Constant pressure heat rejection in the condenser

5- 6: Irreversible throttling in an expansion device

7- 8: Constant pressure heat absorption in an evaporator

An actual vapor-compression refrigeration cycle [25] differs from the ideal one in several ways, owing mostly to the irreversibility that occur in various components, mainly due to fluid friction (causes pressure drops) and heat transfer to or from the surroundings. The COP decreases as a result of irreversibility.

Actual vapor compression cycle differences from ideal one;

- Non-isentropic compression in a compressor
- Superheated vapor state of refrigerant at evaporator exit
- Subcooled liquid at condenser exit
- Pressure drop in condenser and evaporator

T-s diagrams of ideal and actual cycles are shown in Figure 3.4. and 3.5., respectively.

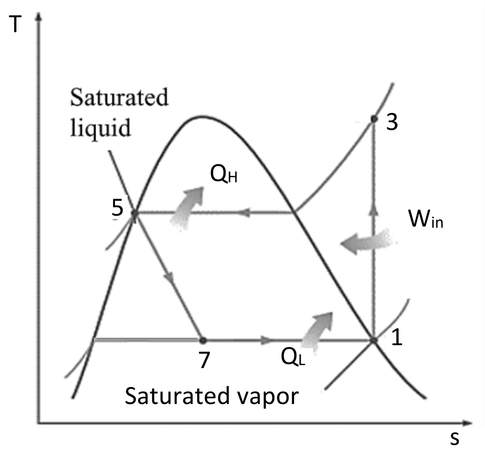

Figure 3.4. T-s Diagram of the ideal vapor-compression refrigeration cycle [25]

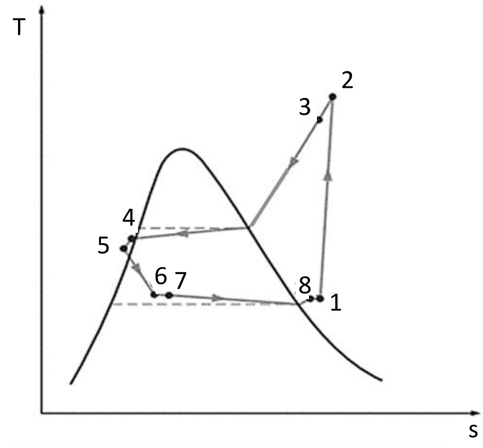

Figure 3.5. T-s Diagram of actual vapor-compression refrigeration cycle [25]

P-h diagrams of ideal and actual cycles are presented in Figure 3.6. and 3.7., respectively.

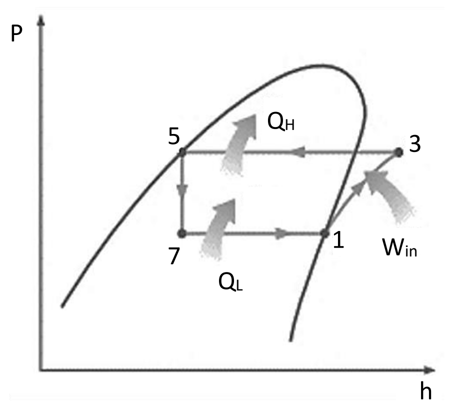

Figure 3.6. P-h Diagram of the ideal vapor-compression refrigeration cycle [25]

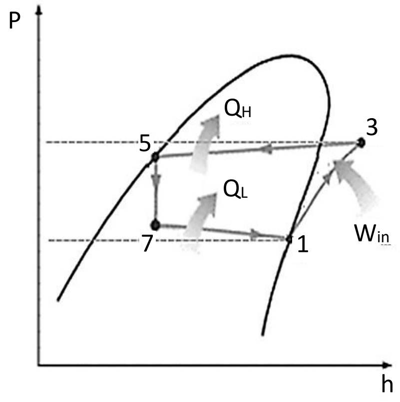

Figure 3.7. P-h Diagram of the actual vapor-compression refrigeration cycle [25]

Shortly, steady-state first law equation for the cycle in specific form can be summarized as:

$$(Q_L - Q_H) + (W_{in} - W_{out}) = 0 \tag{2}$$

$$(COP)_{HP} = \frac{Q_H}{W_{in}} = \frac{h_3 - h_4}{h_2 - h_1} \tag{3}$$

3.2. Heat Pump Components

A heat pump system consists of the following components;

- Evaporator: A heat exchanger in which refrigerant at lower temperature than environment flows. Heat is extracted from ground, air or water to the refrigerant and it evaporates.
- Compressor: It compresses the refrigerant to higher pressure.
- Condenser: A heat exchanger in which excess heat is transferred from refrigerant to the surroundings and the refrigerant condenses.

- Expansion valve: Components in which the refrigerant is expanded resulting in decrease of its pressure.

In the present study, experiment setup is prepared as a prototype domestic dishwasher into which heat pump system is integrated. Heat pump system consists of fans, evaporator, condenser, compressor, capillary and copper tubes. Equipment diagram is shown in Figure 3.8.

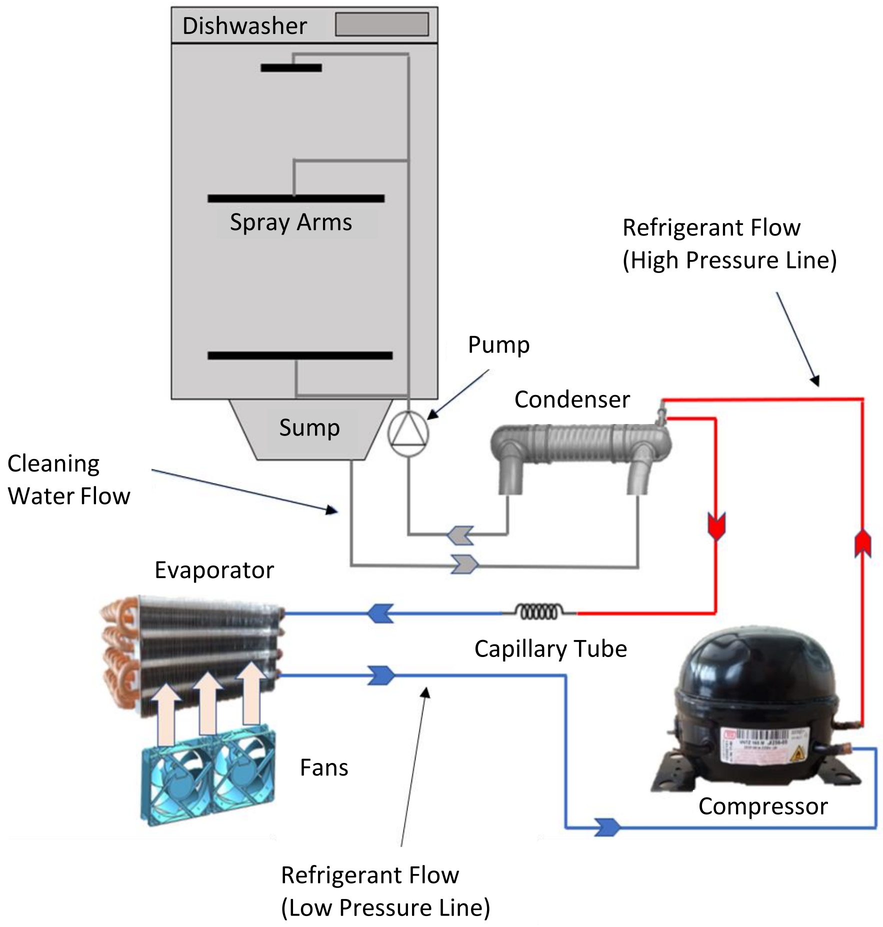

Figure 3.8. Refrigerant flow path diagram of present study

The designed heat pump is presented in Figure 3.9. Oxyacetylene gas welding is used to assembly the components.

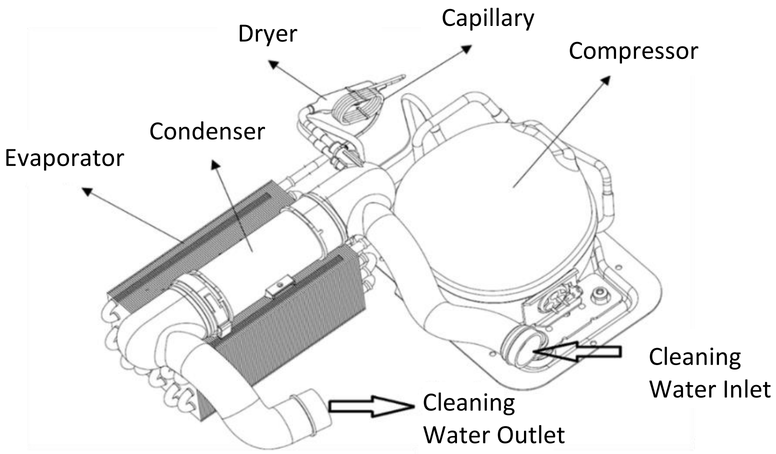

Figure 3.9. Schematic representation of heat pump system assembly

Heat pump system is integrated under the inner tub of dishwasher where most of the electrical and mechanical components are placed. Bottom side of the HPIDW that is used in experiments is shown in Figure 3.10.

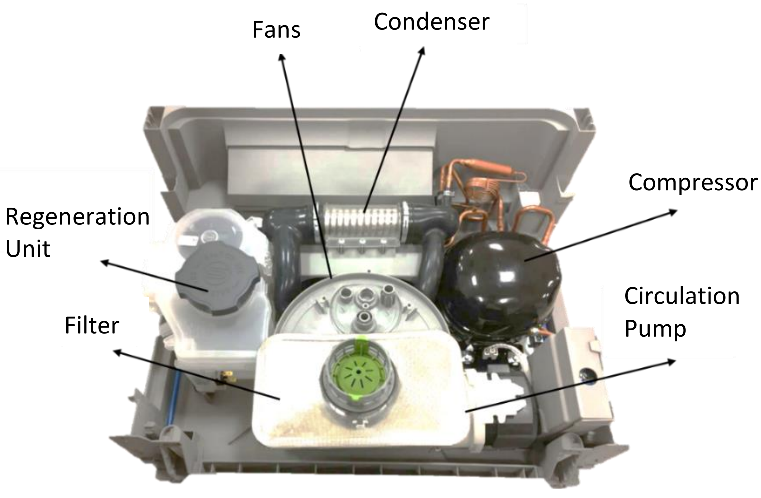

Figure 3.10. Bottom side of HPIDW

The evaporator used in the system is shown in Figure 3.11. Evaporator pipes are made up of copper and aluminum and corrugated fins are inserted.

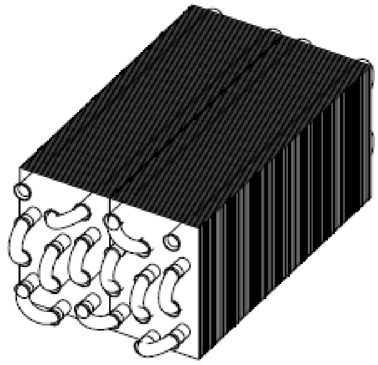

Figure 3.11. 6x4 array configuration evaporator

Stainless steel helical tube which is the condenser in the heat pump system is shown in Figure 3.12. An EPDM case is covered the helical tube. Washing water flows through between outer surface of tube and inner surface of EPDM case. Refrigerant flows inside the tube. Heat is transferred from refrigerant to washing water while heat pump system and circulation pump are working.

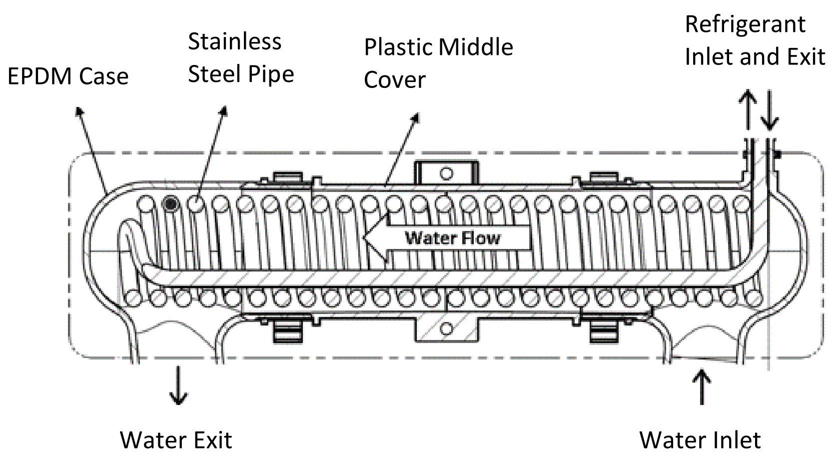

Figure 3.12. Condenser used for heating washing water

Reciprocating type hermetic compressor that is shown in Figure 3.13. is used in order to increase the pressure of refrigerant.

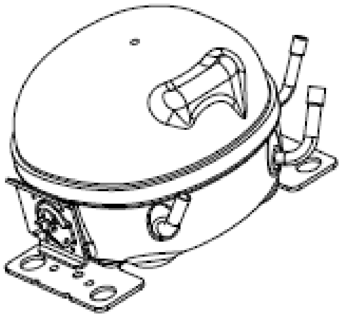

Figure 3.13. Compressor [26]

Capillary tube is used for pressure decrease of the refrigerant before reaching the evaporator. Fluid passes through the dryer which is used for dehumidifying the refrigerant. Two axial dc fans which are shown in Figure 3.14. are located in front of the evaporator to increase heat transfer with forced convection.

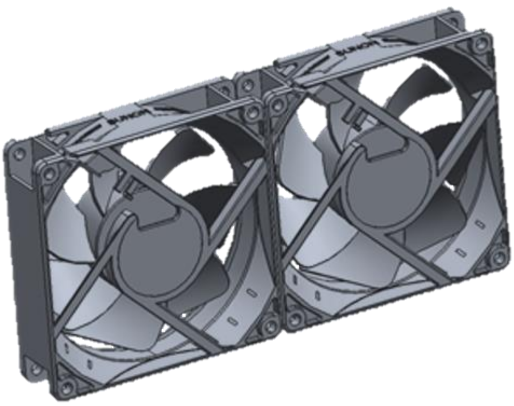

Figure 3.14. Evaporator fans [27]

3.3. Specifications of Heat Pump Components

In the present study, fan and compressor speeds are selected as variables, whereas evaporator and condenser types and capillary tube length are unchanging. Experiments of various coil type evaporators have been conducted, and the one with highest performance is used with considering volume limitation. Condenser is designed with the result of preliminary experiments and CFD analyses within allowed space. Capillary is designed after experiments with varying length and diameter. Fans are selected to achieve higher air flow rate and lower noise level. Because, a novel dishwasher design has been done with integration of heat pump system to a domestic standard size dishwasher and due to volume restrictions only selected variables can be changed.

3.3.1. Evaporator

6x4 array coil type evaporator specifications are given in Table 3.1.

Table 3.1. Evaporator specifications

Material of fins	Aluminum
Material of pipe	Copper
Pipe inlet diameter	6.2 mm
Pipe outlet diameter	7 mm
Fin thickness	0.1 mm
Distance between two fins	1.59 mm
Surface area of a fin	8186.22 mm^2
Total fin number	103 mm^2
Total fin area	843180.80 mm^2
Surface area of pipe	196086.30 mm^2

Array of the evaporator is shown in Figure 3.15. Given dimensions are in mm.

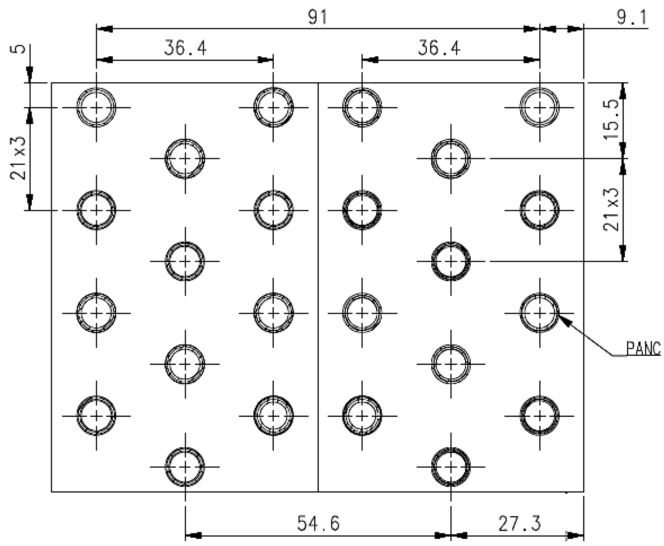

Figure 3.15. Evaporator arrays

Isometric view of evaporator used in the system is shown in Figure 3.16.

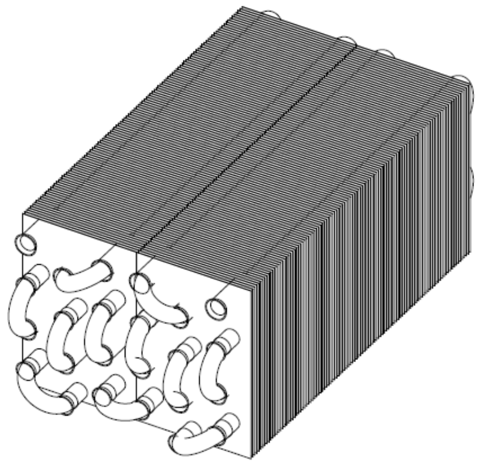

Figure 3.16. Evaporator isometric view

3.3.2. Condenser

Stainless steel condenser is designed for heat pump system. Refrigerant flows in the steel pipe while cleaning water flows outside of the condenser.

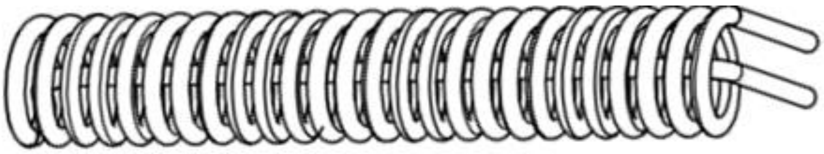

Figure 3.17. Condenser

In thesis study, one standard type condenser is selected and not changed in experiments, therefore there are no analyses stated based on the condenser.

Table 3.2. Condenser specifications

Material of condenser	AISI 316L	
Inlet diameter	6.35	mm
Length	3060	mm

3.3.3. Evaporator Fan

Axial DC fan is used in the heat pump system. The technical specifications are given in the Table 3.3.

Table 3.3. Fan specifications [27]

Rated Voltage	12 VDC
Operating Voltage Range	4.5-13.8 VDC
Rated Current	180 mA
Rated Power Consumption	2.16 W
Air Flow	53.2 CFM
Static Pressure	0.22 Inch-H_2O
Acoustic Noise	37.3 dBA
Rated Speed	3400 rpm ± 10% rated voltage

Air flow and static pressure curve is shown in Figure 3.18.

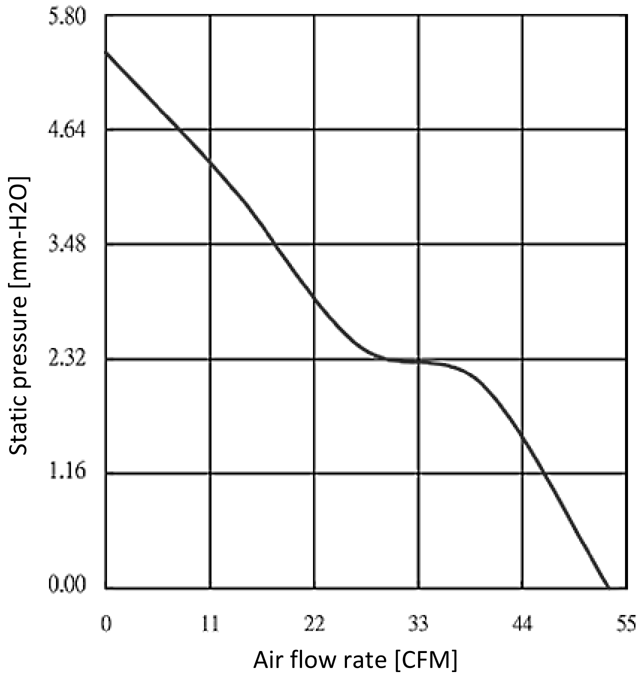

Figure 3.18. Fan characteristic curve [27]

3.3.4. Compressor

Electrical data of compressor is shown in Table 3.4.

Table 3.4. Electrical specifications of compressor [26]

Starting Device	Inverter
Maximum Input Power	235 W
Maximum Input Current	1.4 A
Winding Resistance	11.6 Ohms
Locked Rotor Current	3.0 A
Nominal Input Voltage Range	176 to 264 VAC

Performance characteristics are given according to Ashrae standards at -23.3 °C evaporation and 54.4 °C condensation temperatures in Table 3.5.

Table 3.5. Performance characteristics of compressor [26]

Displacement [cc]	**Output Frequency [Hz]**	**Speed [rpm]**	**Capacity [kcal/h]**	**COP [-]**
11.28	43.3	1300	75	1.70
	100	3000	175	1.74
	150	4500	223	1.60

3.4. Refrigerant

In domestic refrigerators CFCs (chlorofluorocarbon refrigerants) were used widely as working fluid. CFC refrigerants have high level of ozone depletion potential (ODP) and global warming potential (GWP). With the Montreal Protocol [28] agreement in

1987, usage of these refrigerants decreased and limited in years in order to recover ozone layer. With Kyoto Protocol (1997) [29], Montreal Protocol was enhanced to limit usage of hydrochlorofluorocarbons (HCFCs) that contribute global warming.

R134a is commonly used in household appliances as refrigerant since thermodynamic and thermophysical properties are highly suitable. However, its global warming potential (GWP) is 1370 [30] which is high. With Kyoto protocol, it is banned and limited to use. Therefore, conventional refrigerants need to be replaced with low GWP refrigerants.

R600a (isobutane) is selected as working refrigerant in the heat pump system. Due to international regulations gases are classified according to their impact on global warming and ozone layer. R600a is one of the best low GWP alternatives for conventional refrigerants such as R134a, R152a and R12.

Sanchez et al. [31] conducted experimental analysis for comparison of R134a alternative refrigerants with low GWP value. R152a, R1234yf, R1234ze(E), R290 and R600a are tested with consideration of varying operating conditions. In R600a system condensing and evaporating temperature is decreased when comparing with R134a in the same system and conditions. As a result, R600a shows a high level of decrease in cooling capacity and energy consumption because of its low specific volume. Because of this reason, R600a compressor needs a larger displacement to achieve the similar cooling capacity as with R134a.

Hastak et al. [32] conducted experiments on refrigerator systems with R134a, R436a and R600a as refrigerants. Tests were done to analyses the performance of refrigerant and make comparison. Capillary length, compressor and refrigerant amount were varying parameters. As a result, COP of the system was increased by 60.25% with R436a when compared with R134a and 27.11% with R600a. Energy consumption was decreased 41.66% with R436a with respect to R134a and 15.66% with respect to R600a.

Joybari et al. [33] studied the efficiency of R134a and R600a refrigerants comparison with EU Standard EU 1060/2010. Energy efficiency index values and energy labels were compared. According to the standard test method, R600a shows a better performance.

Reddy et al. [34] focused on performance comparison of domestic refrigerator with using R12, R134a and R600a refrigerants. Experiments were conducted in controlled ambient conditions and performance of vapor comparison refrigeration system is investigated. Refrigerant R600a has zero ODP and negligible GWP. However, it is a highly flammable refrigerant. It was observed that R600a has higher COP when compared with other refrigerants.

CHAPTER 4

EXPERIMENTAL PROCEDURE

4.1. General Considerations

In this thesis study, comparative experiments are conducted on electric resistance dishwasher (ERDW) and heat pump system integrated dishwasher (HPIDW). The experiments have been conducted in Arçelik Dishwasher Plant R&D Laboratory. The schematic experimental setups are presented in Figure 4.1. and 4.2., respectively. The aim is to distinguish the energy consumption, operation time and noise level changes with different compressor speeds (N) and air flow rates ($\dot{V}$).

The experiments are performed in a controlled room to simulate inner environment conditions of a typical house as stated in EN 50242 European test standard [23]. The ambient conditions which are maintained and recorded throughout the experiments are presented in Table 4.1.

Table 4.1. Ambient conditions

Ambient room air temperature	23 ± 2°C
Relative humidity	65 ± 10% RH
Supply frequency	50 ± 1% Hz
Supply voltage	230 ± 1% V
Temperature of supplied water	15 ± 2 °C
Water hardness	2.5 ± 0.5 mmol/l
Water supply pressure	240 ± 20 kPa

The reference detergent B is used with an amount of 2.0 g/place setting for dishwashers [23].

4.2. Experimental Setup

In dishwashers, cleaning cycle starts with water intake through water inlet valve. Tap water is directed to regeneration group in which it is softened. After that, water is collected in the sump. Circulation pump is integrated to the sump and used for circulating the washing water through a valve and then spray arms. In the end of each step of cleaning cycle, the dirty water is discharged.

For HPIDW in the present study, the compressor is started when water circulation starts, and the refrigerant is compressed. The pressurized refrigerant reaches to the condenser and its heat is transferred to water. Through the capillary tube the pressure of the refrigerant is reduced and with the help of fans on air side, enhanced heat transfer from air to low pressure refrigerant occurs in the evaporator. In the end of cycle, refrigerant reaches to the inlet of the compressor. Schematic experiment setups of ERDW and HPIDW are figured out in Figure 4.1. and 4.2, respectively.

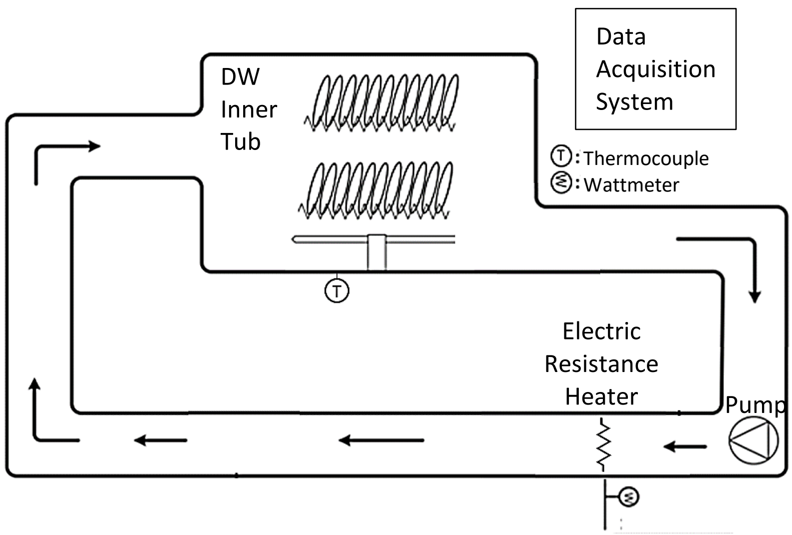

Figure 4.1. Schematic experiment setup of ERDW

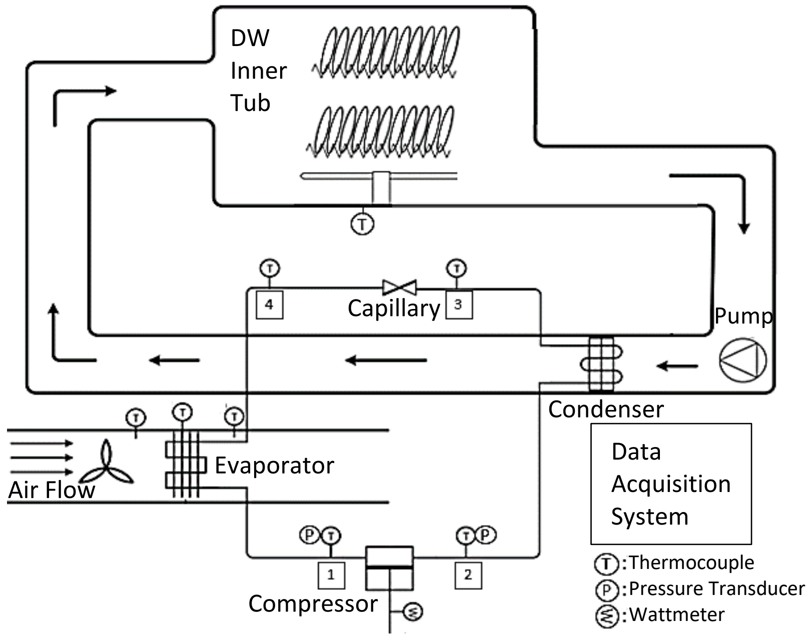

Figure 4.2. Schematic experiment setup of HPIDW

Keysight 34970A [35] datalogger is used for acquiring experimental data. Driving fans and setting of the compressor speed have been achieved by using GW INSTEK GPC-3030D DC [36] power supply and MCP SG1638N [37] signal generator, respectively. The signal generator provides compressor speed with ± 5 rpm fluctuation. Experimental equipments are shown in Figure 4.3.

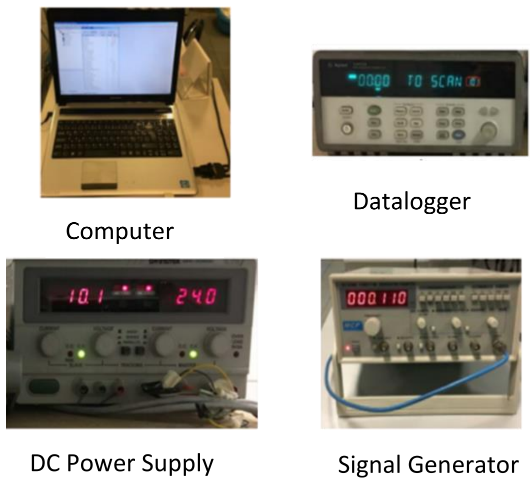

Figure 4.3. Experimental equipments

Dishwasher cabinet is used in the experiments according to the directions in the standards since the designed dishwasher is built-in type as presented in Figure 4.4.

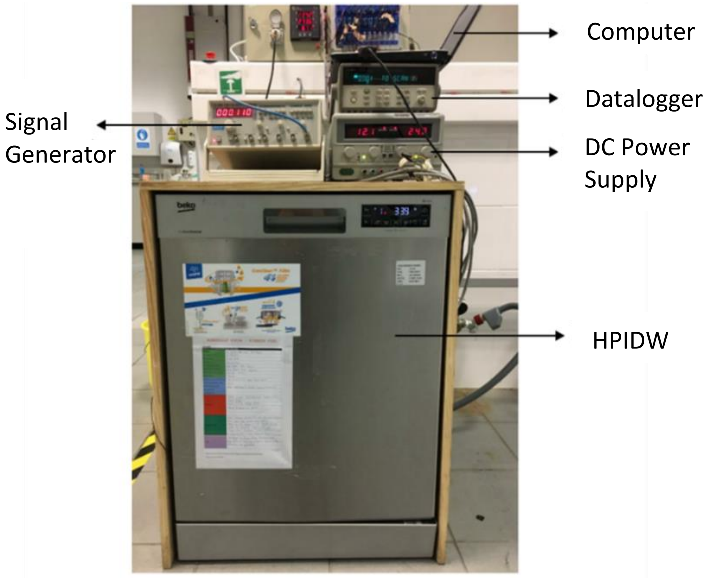

Figure 4.4. Experiment setup

Prototype heat pump system located at the bottom of the dishwasher is shown in Figure 4.5.

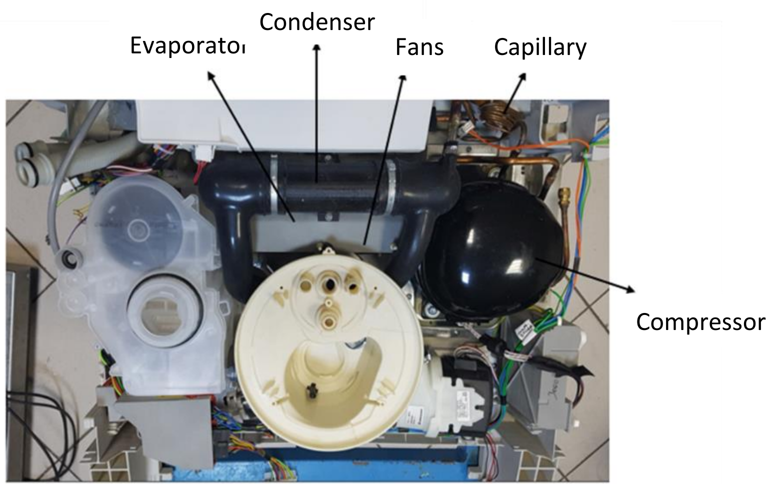

Figure 4.5. Prototype of HPIDW used in experiments

4.3. Experiment Matrix

Reference experiments are done with ERDW. Compressor speed and volumetric air flow rate are varying parameters in experimental matrix. Accepted ranges for these parameters considered in ERDW and HPIDW experiments are summarized in Table 4.2. and 4.3, respectively.

Table 4.2. Air flow rate variables used in experiments

	Compressor Speed (N) [rpm]	Air Flow Rate ($\dot{V}$) [m^3/s]
First Set of Variables	3200 (Constant)	0.016
		0.014
		0.012
		0.010
		0.008

Table 4.3. Compressor speed variables used in experiments

	Compressor Speed (N) [rpm]	Air Flow Rate ($\dot{V}$) [m^3/s]
Second Set of Variables	3500	0.016 (Constant)
	3200	
	2900	
	2600	
	2300	

Experimentation for the determination of energy consumption, operating time and noise level is performed by keeping the first variable (compressor speed) at a value of

3200 rpm and changing the second variable (air flow rate) in between 0.008 m^3/s and 0.016 m^3/s, and vice versa.

Parameter ranges are predetermined considering energy consumption and noise limitations. Solely, the compressor has its best performance around a speed of 3200 rpm, whereas from noise limitation perspective, acceptable maximum value for the air flow rate is determined to be 0.016 m^3/s. Values out of these ranges for the variables lead to worse outputs.

CHAPTER 5

OPTIMIZATION METHODOLOGY

5.1. Multi-Objective Particle Swarm Optimization (MOPSO)

Particle swarm optimization (PSO) is a stochastic optimization method based on population introduced by Dr. Eberhart and Dr. Kennedy in 1995, influenced by bird flocking or fish schooling social behavior [38], [39].

In PSO, the possible solutions are obtained by traveling through the problem space by tracking the present optimum particles. In the problem space, each particle keeps track of its coordinates connected with the best solution that has accomplished up to this point. This value is introduced as ***pbest***. Whenever a particle gets the best value in entire population, its location is a global best and called ***gbest***.

At each time step, the particle swarm optimization concept consists of changing the velocity of each particle toward its pbest and gbest locations. Acceleration is weighted by a random term, with separate arbitrary numbers being generated for acceleration toward pbest and gbest locations.

PSO has been effectively implemented in many fields of research areas in recent years [17]. It is shown that PSO has a quicker, cheaper way of achieving better outcomes compared to other methods. PSO is also useful because there are few variables which need to be changed. Therefore, it has been used for methods that can be used across a wide range of applications.

There is a multi-objective version of PSO named as MOPSO that incorporates the Pareto Envelope and grid making method, similar to Pareto Envelope-based Selection Algorithm to solve the multi-objective optimization problems. Like PSO, MOPSO particles share data and move to the finest global particles their finest local memory.

On the other hand, unlike PSO, the best value is defined and determined by more than one factor. All non-dominated particles in the swarm are collected into a sub-swarm called as ***repository***, and each particle selects its best global target among this repository's particles. Domination-based and probabilistic models are used for the finest local particle.

In order to perform optimization, objective functions are selected. There are three objective functions that needs to be minimized; energy consumption, operating time and noise level. Experimental data from the results of experiment matrix mentioned in Chapter 4.3 are used to create objective functions. Polynomial curve fit equations are obtained from the results of experiments and the curve fit equations are used as objective functions. In these functions, compressor speed and air flow rate are the parameters since the experiments are conducted with-them. Multi-objective particle swarm algorithm is executed and pareto fronts for three objectives are obtained. Determined objective functions are given in Chapter 6.2.

MOPSO algorithm defined by Coello [18] is used for better search capability in the space to deal with multi objective optimization with constraints. With the advantage of PSO, lower computational times are required to achieve optimization results. The flowchart of the algorithm is given in Figure 5.1.

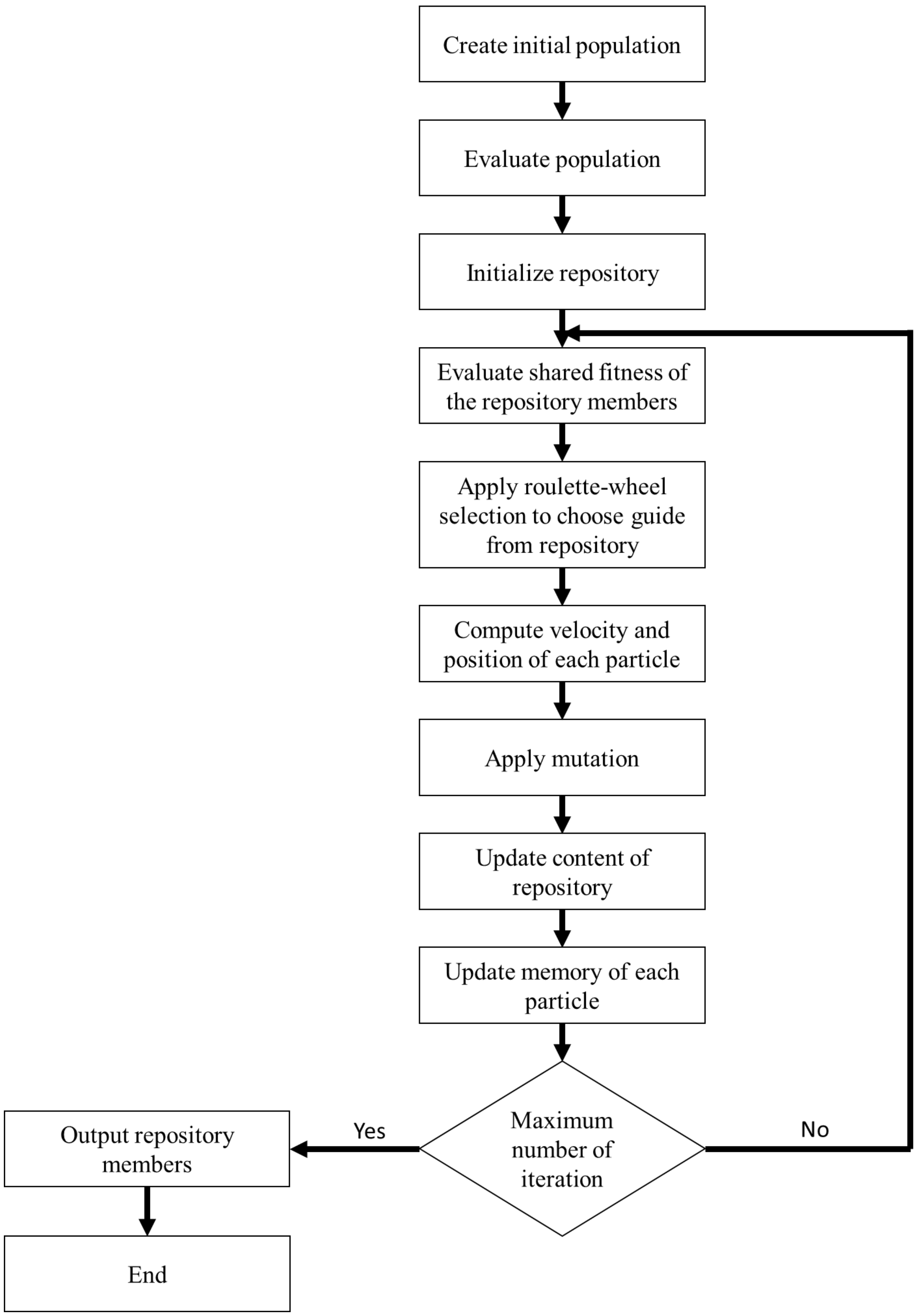

Figure 5.1. Flowchart of multi-objective particle swarm optimization, MOPSO

5.2. Why MOPSO?

Genetic Algorithm (GA) and Particle Swarm Optimization (PSO) methods are mainly used for optimization of constrained and unconstrained problems in the literature [40].

Evolutionary algorithm (EA) is a subgroup of evolutionary computation, a population-based metaheuristic optimization method [41]. An EA utilizes mechanisms inspired by genetic evolution and natural selection.

GA is the most common form of EA. The genetic algorithm continuously modifies individual solutions in order to find a better solution. At each iteration, individuals are chosen randomly to be parents and to create the next generation. After some generations, the population converges to an optimal solution. The primary benefit of the genetic algorithm is that it can be applied to a wide range of problems such as non-linear, non-differentiable and discontinuous problems.

The strength of GAs is the genetic operators used for the search [40]. Crossover operator attempts to preserve the beneficial aspects of candidate solutions and to eliminate undesirable components. Mutation operator is likely to degrade a strong candidate solution than to improve it. By restricting the reproduction of weak candidates, GAs eliminate that solution with its descendants. It makes the algorithm converge towards high quality solutions within a few generations.

Particle Swarm optimization (PSO) contains many similarities with the methods of Evolutionary Computation (EC) and GAs [42]. All these techniques consider a group of a randomly generated population and use a fitness value to evaluate the population. The main difference between the PSO approach compared to EC and GA is that PSO does not have genetic operators such as crossover and mutation. Particles update themselves with the internal velocity; and they also have a memory which is very important for the algorithm. Additionally, in PSO only the best particle reflects information to others. It is a one-way information sharing mechanism in which the evolution only searches for the best solution. Compared to GAs, PSO is easy to be implemented and there are few parameters to adjust.

The computational effort required for PSO to reach such high quality solutions is less than that of GAs [43].

Elbeltagi et al. [44] conducted a research about five evolutionary-based search algorithms; Genetic Algorithm (GA), Memetic Algorithm (MA), Particle Swarm Optimization (PSO), Ant Colony Optimization (ACO), and Shuffled Frog Leaping (SFL). Visual Basic codes were implemented to apply optimization algorithms. Continues and discrete problems were solved, and the comparative results were given. The PSO method was generally found to perform better than other algorithms in terms of success rate and solution quality, while being the second in terms of processing time.

CHAPTER 6

RESULTS

6.1. Experimental Results

6.1.1. Standard Energy Consumption Experiments for ERDW

Experiments for electric resistance domestic dishwasher (ERDW) with an energy efficiency of A+++ are performed according to European Standard EN50242 [23]. Eco program, which is selected in the experiments, is developed and optimized on the product up to now.

For comparison, firstly experiment of 1800 W resistance heater dishwasher has been conducted. The results show that ERDW consumes 853 Wh energy with the heater as the main source of this consumption. During main washing, hot rinsing, cold rinsing and drying steps energy consumptions are 553 Wh and 249 Wh, 15 Wh and 36 Wh, respectively. Change in water temperature and energy consumption with time is shown in Figure 6.1.

In the cold rinse and drying steps, electrical heater does not work, whereas in the cold rinse step only circulation pump runs. Similarly, in the drying step only drying fan works. Circulation pump and drying fan consume 48 W and 20 W, respectively. The major energy consumption source is the heater. Also, main wash and hot rinse durations are quite longer than cold rinse step. As a result, cold rinse and drying steps do not have a noticeable effect on total energy consumption.

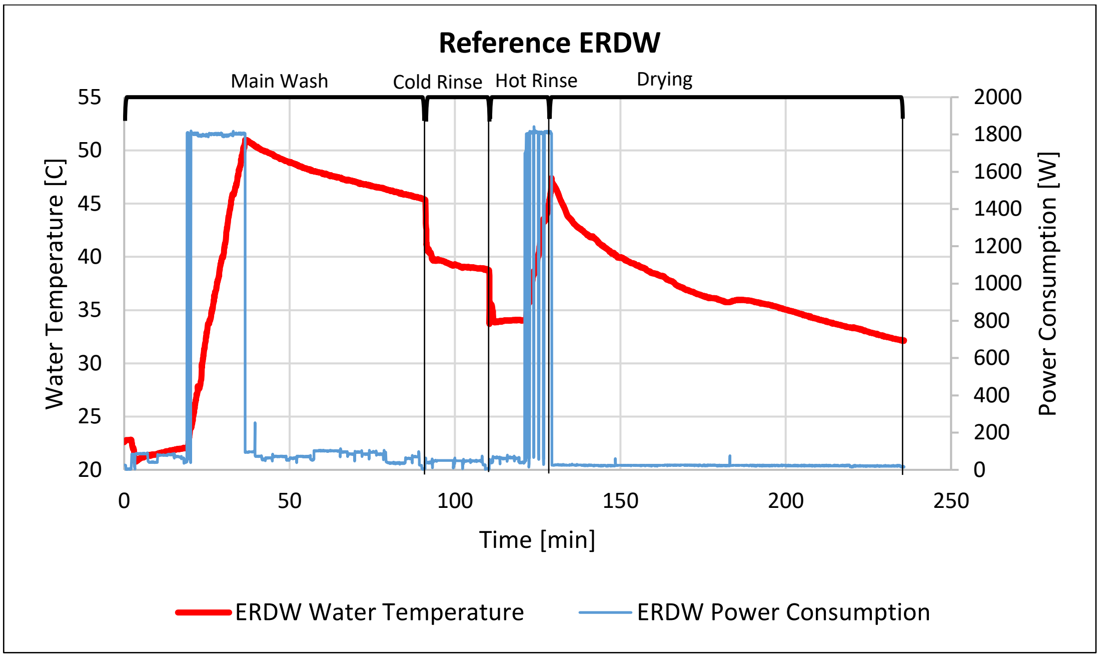

Figure 6.1. Energy consumption and temperature change of reference dishwasher during eco cleaning program

Total dishwasher operating time is 235 mins. The diffraction of energy consumption and operation time are presented in Table 6.1.

Table 6.1. Energy consumption and operating time of ERDW

	Operating Time (t) [min]	**Energy Consumption (E) [Wh]**
Main wash	91	553
Cold rinse	19	15
Hot rinse	20	249
Drying	105	36
Total	235	853

Noise level is measured as 43.3 dBA in dishwasher acoustic test according to IEC 60704-2-3 [45].

6.1.2. Comparable Experimental Results of ERDW and HPIDW

After heat pump installation to the dishwasher, energy consumption and acoustic characterization experiments are repeated. HPIDW experiments are conducted with 3500 rpm compressor speed, as explained in section 4.3, Experiment matrix. Air flow rate is kept constant at a value of 0.016 m^3/s in order to compare compressor speed effect on energy consumption, noise level and heating time.

In HPIDW experiments, heat pump system and fans are operated instead of electric resistance. All the other components like circulation pump, drain pump, valve etc. do work identically in both HPIDW and ERDW experiments.

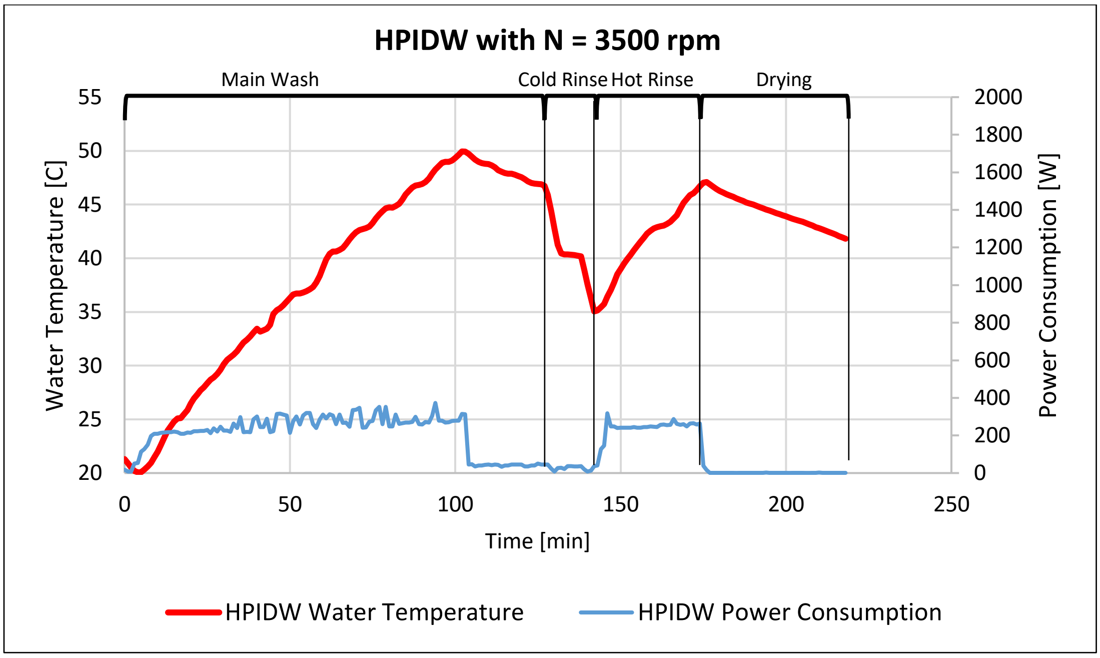

Figure 6.2. Energy consumption and temperature change of HPIDW during eco cleaning program

Water temperature change and energy consumption with time are shown in Figure 6.3. for both ERDW and HPIDW systems.

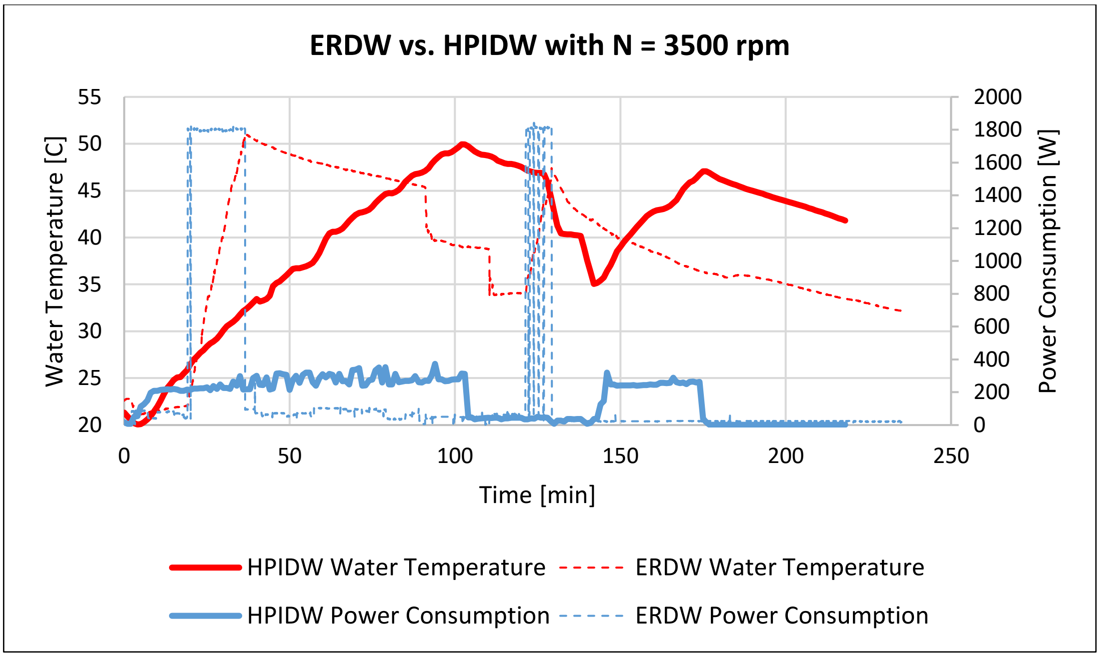

Figure 6.3. Energy cons. and temperature change of water for ERDW and HPIDW – 3500 rpm

For 3500 rpm compressor speed; the maximum noise level in HPIDW system is measured as 47.8 dBA. Energy consumption of the eco cleaning program is 587 Wh, whereas the time consumption is recorded as 217 min. Consumed energy in HPIDW system is 266 Wh lower than that of the ERDW. Necessary time to complete main wash step is increased at about 38 min. Noise level is also increased by 4.5 dBA due to compressor and fans.

Increase of main wash duration leads to better cleaning performance at this first step. As a result, cold rinse duration is decreased in order to compensate total operating time by keeping the cleaning quality the same with performing related tests continuously. HPIDW experiments are conducted with modified cleaning program considering new cold rinse duration which does not create a major difference in total energy consumption, since both resistance heater and heat pump system do not work in the cold rinse step. Similarly, shortening the drying duration in HPIDW does not affect energy consumption of it. As drying system, ERDW has a fan which sucks the humid air from the dishwasher. The system decreases the relative humidity of air inside the dishwasher by mixing it with relatively dry ambient air resulting in better drying performance. In HPIDW, since there is not enough volume left for a drying fan due to limited space, drying is enhanced with automatic door opening process within the 5th minute of drying step. Although automatic door opening mechanism cost is high, it shortens drying duration. With these reasons, energy consumption has not been affected from duration of drying in HPIDW while reaching the same drying performance.

Comparison of performance characteristics of HPIDW with ERDW system at compressor speeds of 3200, 2900, 2600 and 2300 rpm are presented in Figure 6.4. – 6.7.

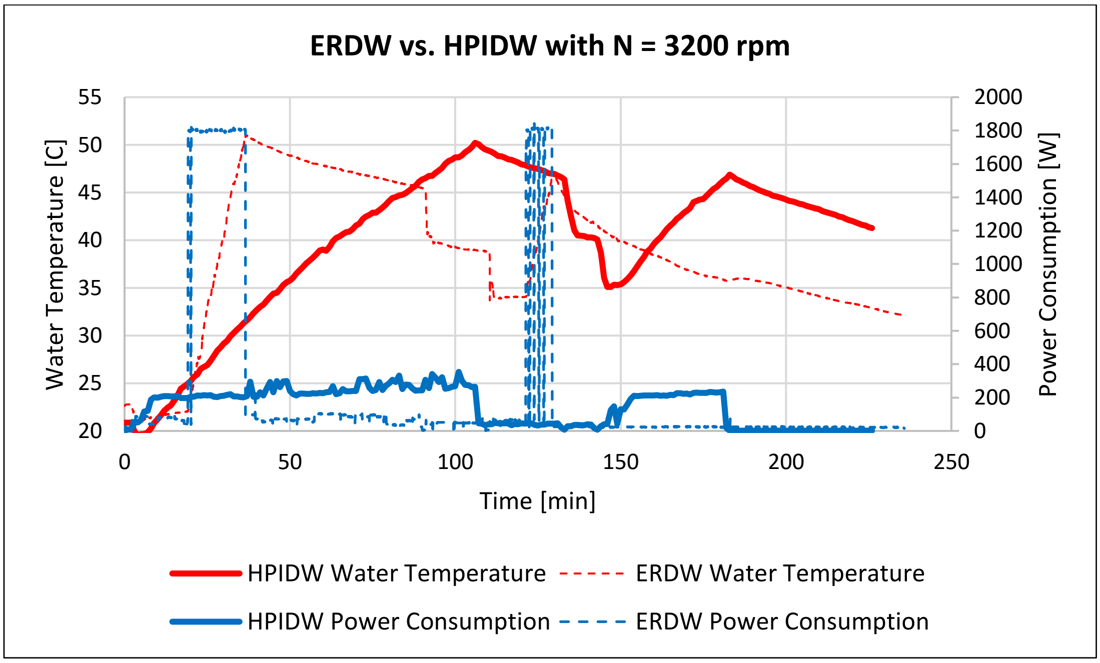

Figure 6.4. Energy cons. and temperature change of water for ERDW and HPIDW – 3200 rpm

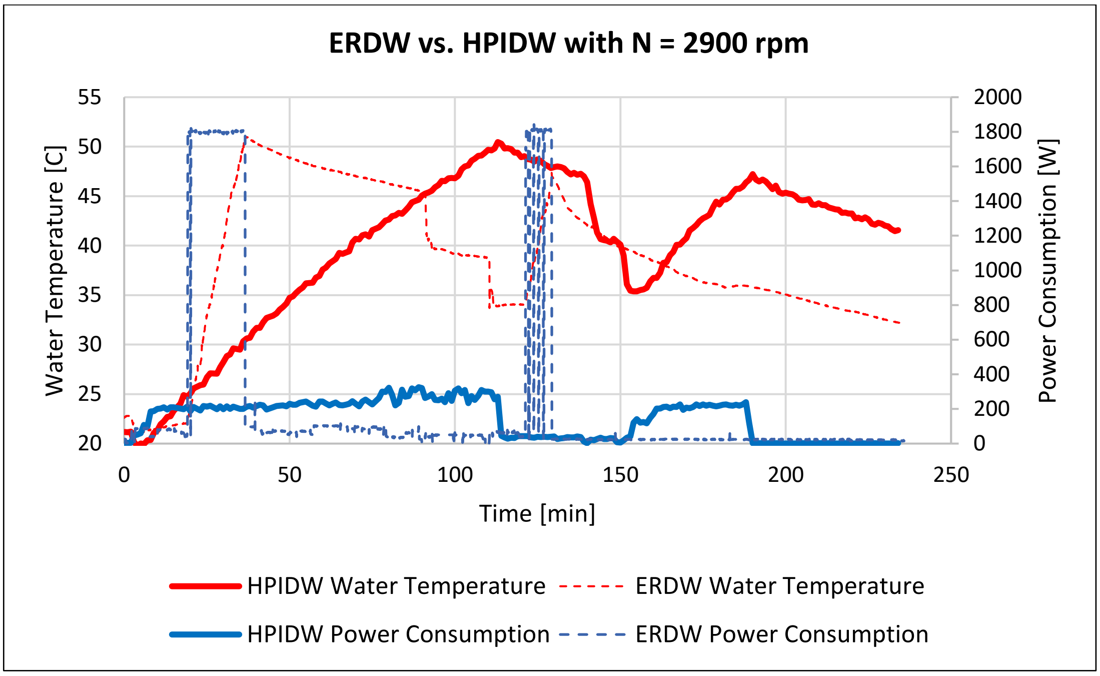

Figure 6.5. Energy cons. and temperature change of water for ERDW and HPIDW – 2900 rpm

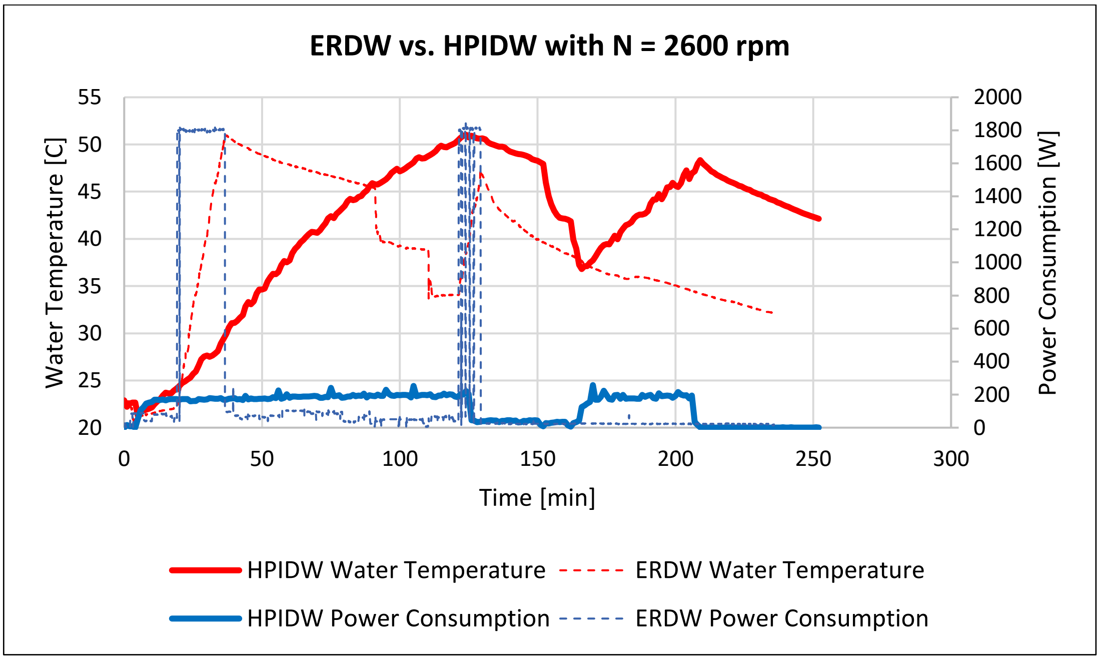

Figure 6.6. Energy cons. and temperature change of water for ERDW and HPIDW – 2600 rpm

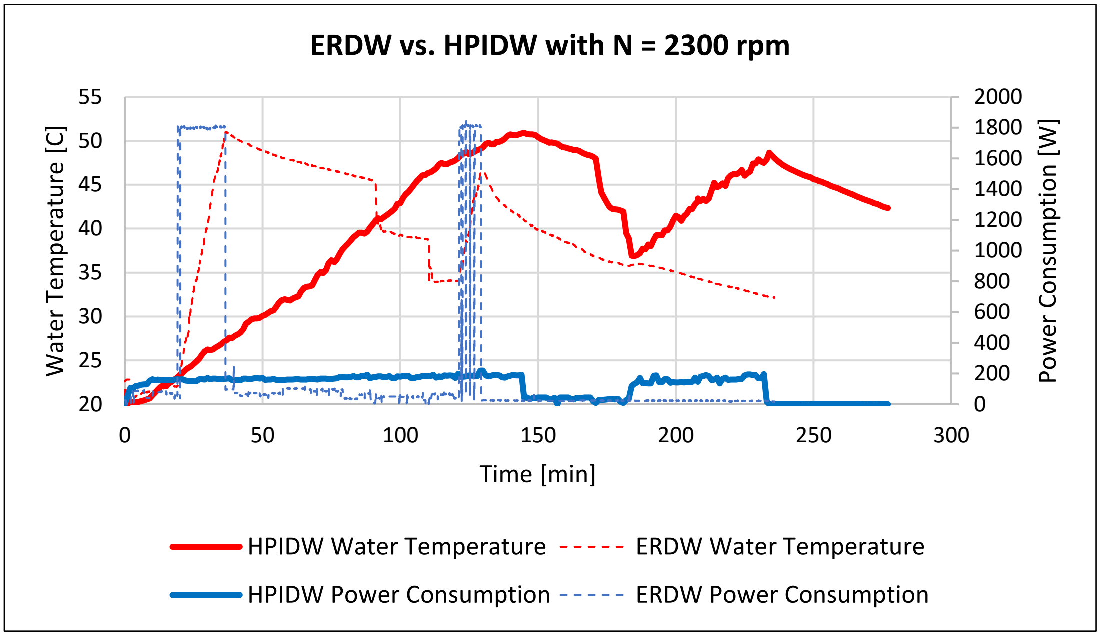

Figure 6.7. Energy cons. and temperature change of water for ERDW and HPIDW – 2300 rpm

When figures are examined it is observed that the energy consumption decreases as compressor speed is reduced down to 2600 rpm. However, energy consumption increases at compressor speed values below 2600 rpm. The reason is that below certain speed, there is an excessive increase in working duration. In HPIDW system, energy consumption is reduced up to 521 Wh when compared to ERDW system. As expected; heating time shortens with the increase in compressor speed. In HPIDW system, main wash heating time is up to 81 minutes longer than ERDW system. Noise level falls down with decreasing compressor speed. On the other hand; there is about 3.8 dBA increase in the maximum noise level of HPIDW when compared to ERDW system.

Highlights of the experimental results for varying compressor speed and constant air flow rate are presented in Table 6.2. Results for dishwasher operating time and noise level are tabulated in Table 6.3. and 6.4, respectively.

Table 6.2. Energy consumption results for varying compressor speeds

Energy Cons. (E) [Wh]	ERDW	HPIDW *3500 rpm*	HPIDW *3200 rpm*	HPIDW *2900 rpm*	HPIDW *2600 rpm*	HPIDW *2300 rpm*	$\dot{V}$ = 0.016 m^3/s
Main wash	553	447	425	395	384	418	
Cold rinse	15	5	5	5	5	5	
Hot rinse	249	135	125	128	132	138	
Drying	36	0.8	0.8	0.8	0.8	0.8	
Total	853	587	555	528	521	561	

Table 6.3. Dishwasher operating time data for different compressor speeds

Operating Time (t) [min]	ERDW	HPIDW *3500 rpm*	HPIDW *3200 rpm*	HPIDW *2900 rpm*	HPIDW *2600 rpm*	HPIDW *2300 rpm*	$\dot{V}$ = 0.016 m^3/s
Main wash	91	129	133	140	151	172	
Cold rinse	20	10	11	10	9	9	
Hot rinse	19	38	42	44	48	55	
Drying	105	40	40	40	40	40	
Total	235	217	226	234	252	277	

Table 6.4. Noise level experiment results with change of compressor speed

Comp. Speed (N) [rpm] ($\dot{V}$ = 0.016 m^3/s)	DW Noise Level (A) [dBA]
3500	47.8
3200	47.5
2900	47.3
2600	47.2
2300	47.1
ERDW	43.3

In the main wash and hot rinse steps, the cleaning program algorithm is temperature limit controlled. However, for cold rinse and drying steps, time limit is set. Duration fluctuations in the cold rinse steps are mainly caused by slight instabilities in water taking process and dishwasher mainboard time control algorithm. The fluctuations do not affect energy consumption.

Similar analyses have been performed by keeping the compressor speed constant at 3200 rpm. For constant compressor speed 3200 rpm, energy consumption is measured for 0.008, 0.010, 0.012, 0.014 and 0.016 m^3/s air flow rate values. The results are summarized in Table 6.5.

Table 6.5. Total energy consumption data for different air flow rates

Air Flow Rate ($\dot{V}$) [m^3/s]	**Energy Consumption (E) [Wh]**	
0.008	642	**N = 3200 rpm**
0.010	594	
0.012	567	
0.014	562	
0.016	556	
ERDW	853	

While the compressor speed is kept constant, with increasing air flow rate; operating time and energy consumption values are continuously decreasing. This is so because heat transfer to the refrigerant in the evaporator increases, specific compressor work remains the same and heat transfer to the water at condenser increases resulting in shorter heating time and lower total energy consumption. Increase in the air flow rate is achieved by rising the fan speed which leads to higher measured noise level values.

Table 6.6. Dishwasher operating time data for different air flow rates

Air Flow Rate ($\dot{V}$) [m^3/s]	Main Wash Duration [min]	Operating Time (t) [min]	
0.008	163	264	**N = 3200 rpm**
0.01	151	252	
0.012	143	239	
0.014	138	230	
0.016	133	226	
ERDW	91	235	

Main wash step and total operating time are recorded and shown in Table 6.6, and noise level results are tabulated in Table 6.7.

Table 6.7. Noise level data for different air flow rates

Air Flow Rate ($\dot{V}$) [m^3/s] (N = 3200 rpm)	DW Noise Level (A) [dBA]
0.016	47.5
0.014	45.9
0.012	45
0.01	44.5
0.008	44.2
ERDW	43.3

All experiment results are systematically presented in Table 6.8. In the matrix, results of experiments for variables are shown in green. Experiment is not conducted for the rest of variables and shown as NA.

Table 6.8. Experiment result matrix

Compressor Speed (N) [rpm]	Air Flow Rate ($\dot{V}$) [m³/s]: 0.008	0.010	0.012	0.014	0.016
3500	E: NA t: NA A: NA	E: NA t: NA A: NA	E: 598 Wh t: 226 min A: 45.4 dBA	E: NA t: NA A: NA	E: 587 Wh t: 217 min A: 47.8 dBA
3200	E: 642 Wh t: 264 min A: 44.2 dBA	E: 594 Wh t: 252 min A:44.5 dBA	E: 567 Wh t: 239 min A: 45.0 dBA	E: 562 Wh t: 230 min A: 45.9 dBA	E: 555 Wh t: 226 min A: 47.5 dBA
2900	E: NA t: NA A: NA	E: NA t: NA A: NA	E: 553 Wh t: 243 min A: 44.8 dBA	E: NA t: NA A: NA	E: 528 Wh t: 234 min A: 47.3 dBA
2600	E: NA t: NA A: NA	E: NA t: NA A: NA	E:543 Wh t: 260 min A: 44.7 dBA	E: NA t: NA A: NA	E: 521 Wh t: 252 min A: 47.2 dBA
2300	E: NA t: NA A: NA	E: NA t: NA A: NA	E: 593 Wh t: 284 min A: 44.6 dBA	E: NA t: NA A: NA	E: 561 Wh t: 277 min A: 47.1 dBA

If unmodified cold rinse duration (20 mins.) and fan drying system (105 mins. drying time) were assumed to be used in HPIDW, the corresponding energy consumption values for these steps would be equal to those in ERDW. In this case; for HPIDW, energy consumption could be reduced up to 567 Wh, whereas minimum 292 min operating time can be reached. Comparable results for energy consumption and operating time are shown in Table 6.9.

Table 6.9. Unmodified cleaning program comparison

	ERDW	**HPIDW** ***3500 rpm***	**HPIDW** ***3200 rpm***	**HPIDW** ***2900 rpm***	**HPIDW** ***2600 rpm***	**HPIDW** ***2300 rpm***	
Energy Cons. (E) [Wh]	853	633	601	574	567	607	**$\dot{V}$ = 0.016 m^3/s**
Operating Time (t) [min]	235	292	300	309	324	352	

6.2. Uncertainty Analyses

Uncertainty analyses have been done to determine the error in the experiments. Calculations are performed as suggested in IEC Guide 115 Application of Uncertainty of Measurement to Conformity Assessment Activities in the Electrotechnical Sector [46]. It is shown in Table 6.9. that, uncertainty in energy consumption experiment is calculated as 3.9% with level of confidence 95%.

The uncertainty is carried out using the manufacturers' specifications which is defined as category B evaluation in the literature [47]. Since manufacturers' specification limits are used as the uncertainty, rectangular distribution is assigned.

The T type thermocouple [48], Liebert Emerson Precision Air Conditioner [49], Liebert NX UPS Power Regulator [50] and MPR-535-96 Power Analyzer [51] are the main sources of uncertainty and related values of uncertainties for these are taken considering their manufacturers' specifications.

Table 6.10. Uncertainty characteristics

Source of Unc.	**Cat.**	**Error Qty. Sp(X_i)**	**Probability Shape**	**Dist. Division Factor**	**Standard Unc. u(X_i)**	**Unc. Contribution u_i(y)**
Thermocouple	B	0.75%	Rectangular	1.73	0.43%	0.43%
Relative Humidity	B	2.00%	Rectangular	1.73	1.15%	1.15%
Line Voltage	B	0.76%	Rectangular	1.73	0.44%	0.44%
Frequency	B	0.02%	Rectangular	1.73	0.01%	0.01%
Preparing	B	1.00%	Rectangular	1.73	0.58%	0.58%
Wattmeter	B	1.00%	Rectangular	1.73	0.58%	0.58%
Water Usage	B	2.00%	Rectangular	1.73	1.15%	1.15%
					Combined Uncertainty U_c=(Sum $u_i^2)^{-2}$	1.93%
					Coverage Factor (Kp) [Level of confidence: 95%=2]	2
					Expanded Uncertainty (U)	**3.9%**

For the noise level experiment, uncertainty calculation is conducted as suggested by IEC 60704-2-13 International Standard [52]. The uncertainty arises from nature of sound field of the source, disturbances, absorption of the source under test and the type of intensity field sampling and measurement procedure employed.

The equipments used in noise measurements are Bruel&Kjaer Analyzer (type 7537 and 3039 module) [53] and Bruel&Kjaer Microphone (6 microphones, type 4188) [54]. The estimated values of standard deviations of sound power levels in noise experiments are determined according to the standard are indicated in Table 6.11.

Table 6.11. Standard deviations of sound power levels in noise experiment

Standard Deviation [dBA]	
σ_r – repeatability	σ_R – reproducibility
0.4	0.7

Total standard deviation is calculated as σ_{tot} = 0.81 dBA. Expanded uncertainty with confidence level of 95% is obtained as 1.62 dBA.

6.3. Analytical Validation

In order to verify the experimental results; energy consumption of heat pump system is calculated from thermodynamic heat pump cycle analyses and compared with measured values.

With the help of data acquisition system (DAS); pressure and temperature values of the refrigerant at corresponding inlet and exit states of the heat pump components, the properties of air in cross flow on the outer surface of the evaporator and tank water temperature values are measured and recorded at 60-second-interval. Temperature and pressure data recorded by DAS are used in the state determination of refrigerant in order to perform cycle analyses. P-h diagram of R600a is used [55]. State 2 shown in Figure 4.2. is directly determined from temperature and pressure information. The heat transfer processes in condenser and evaporator are assumed to be at constant pressure. Throttling process in capillary tube is simulated as constant enthalpy process. Since in the beginning of heating process, refrigerant is two phase mixture, using Eqn. 4, state 1 is fixed assuming all heat supplied by air is transferred to the refrigerant flowing inside the evaporator. Specific volume and enthalpy values at saturation and superheated states are determined using predefined equations [56]. For subcooled region, state property values are determined using P-h diagram. Cycle behavior with working time is presented in Figure 6.8.

$$\dot{Q}_{air} = \dot{V} * C_{p,air} * \rho_{air} * \Delta T_{air} \tag{4}$$

Mass flow rate of refrigerant is found using equations available in literature [57].

$$\dot{m} = \frac{N * \eta_V * V_P}{\upsilon_1 * 60} \tag{5}$$

In Eqn. 5, N is compressor speed in rpm, υ_1 is the specific volume of the sucked refrigerant in m^3/kg and η_v is the overall volumetric efficiency and found using Eqn. 6 [55].

$$\eta_V = (1 + C) * \left(\frac{P_s}{P_l}\right)^{\frac{1}{n}} - C * \left(\frac{P_d}{P_l}\right)^{\frac{1}{m}} - f_{leakage} * \left(\frac{P_d}{P_s}\right) \tag{6}$$

In Eqn. 6, lower working pressure (P_l) is evaporator pressure of the ideal refrigeration cycle. $f_{leakage}$ is conventionally assumed to be 0.01. C is the clearance factor and assumed as 0.05, n and m are the index of polytropic compression and re-expansion, respectively. Suction pressure (P_s) and discharged pressure (P_d) are calculated using Eqn. 7 and 8 [57].

$$P_s = P_l * f_{ps} \tag{7}$$

$$P_d = {}^{P_h}\!/_{f_{pd}} \tag{8}$$

where, f_{ps} is the pressure fraction through suction valve, f_{pd} is the pressure fraction through discharge valve and is generally about 0.95. Higher working pressure (P_h) is condenser pressure of the ideal refrigeration cycle.

Swept volume (V_P) which is the volume between top dead center and bottom dead center is calculated with Eqn. 9 [57].

$$V_P = \frac{\pi * D^2}{4} * L \tag{9}$$

Stroke (L) is the distance between bottom dead center and top dead center of the compressor piston. Bore (D) is the diameter of the compressor cylinder.

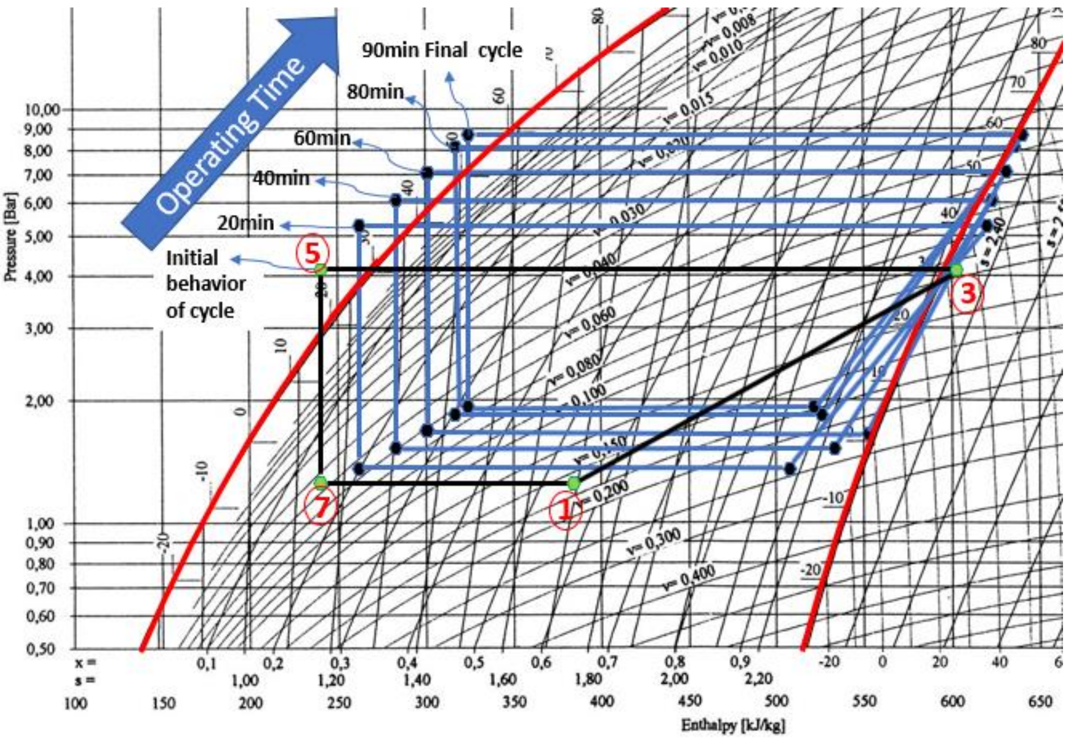

Figure 6.8. P-h Diagram of HPIDW operating time

During main wash step, cycle behavior and corresponding states 1, 3, 5 and 7 are shown within 20 min intervals in Fig. 6.8. After heat pump system starts, condensation and evaporation temperatures and pressures are increasing in time.

Power supplied by the compressor is calculated using Eqn. 10.

$$\dot{W} = \dot{m} * (h_2 - h_1) \tag{10}$$

Total energy consumption is determined by integrating the power supplied by the compressor on operation time. Sample calculation is presented in Appendix A.

Energy consumption of heat pump during main wash heating step is calculated and the results are reflected in Table 6.12.

Table 6.12. Energy consumption comparison between experiment and analytical analyses

Compressor Speed (N) [rpm]	2300	2600	2900	3200	3500
Energy Consumption (E) (Experiments*) [Wh]	368.7	364.7	373.0	402.0	419.3
Energy Consumption (E) (Analytical Analyses) [Wh]	379.1	354.8	360.6	413.3	430.6
Absolute Error Percentage [%]	2.82	2.73	3.32	2.81	2.70

*Pump energy consumption values are extracted.

Considering uncertainty in the experiments, the error percentages shows that the experiment results are reliable.

6.4. MOPSO Results for Heat Pump Cycle Parameters

An optimization study has been done with the parameters of fan and compressor speed. Compressor speed is varying in between 2300 rpm and 3600 rpm. Fan speed is diversed with different supplied voltage of the DC fans so that the air flow rate is changed from 0.008 m^3/s to 0.016 m^3/s. As objectives, dishwasher operating time, noise level and energy consumption values are tried to be minimized.

Multi objective particle swarm optimization method considering three objective functions is used in MATLAB software for optimization. Objective functions are obtained using 3200 rpm constant compressor speed and 0.016 m^3/s constant air flow rate experiments' results which are tabulated in Table 6.9. On the other hand, 0.012 m^3/s constant air flow rate experiment results are used to check validity of objective functions.

Polynomial regression analyses are performed to relate dependent variables (energy consumption, operating time and noise level) as 2^{nd} or 3^{rd} order polynomials of independent variables (compressor speed and air flow rate).

Using the results data of the energy consumption experiments, 3^{rd} order polynomial regression line is obtained as presented in Figure 6.9 and curve fit equation of energy consumption (E) in terms of compressor speed (N) is obtained.

Similar analyses have been done for operating time and noise level data and 2^{nd} order polynomial regression lines are obtained using Figure 6.10 and 6.11, respectively.

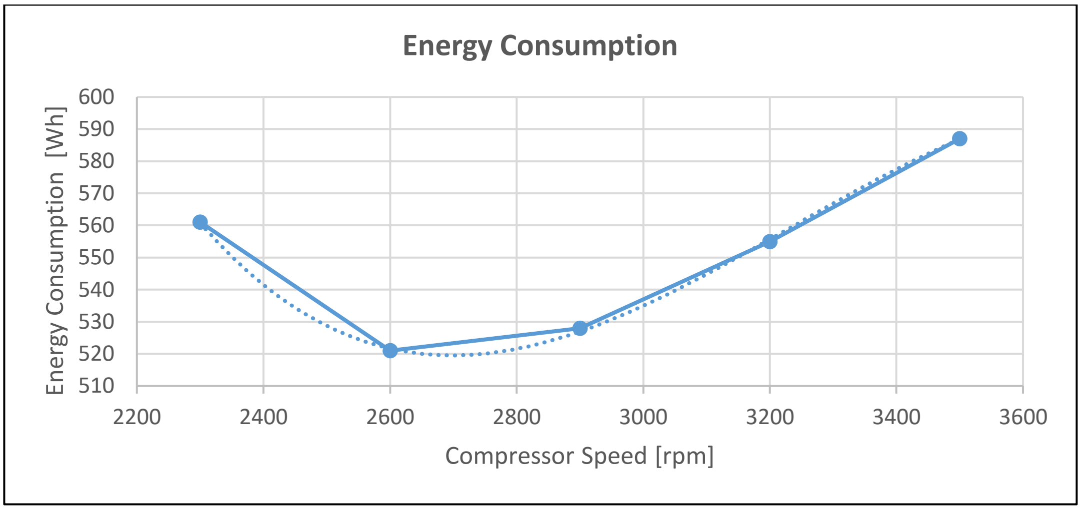

Figure 6.9. Energy consumption curve fit

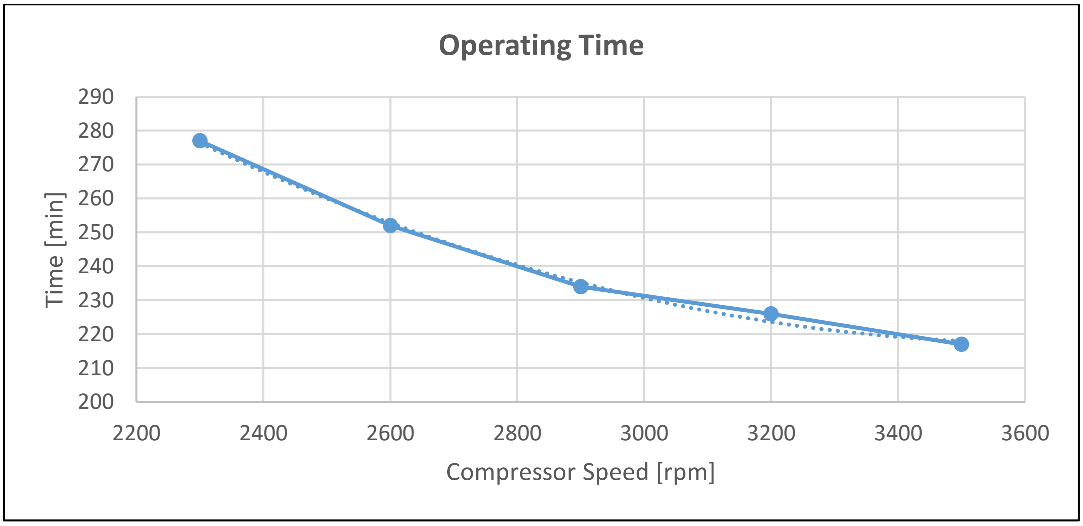

Figure 6.10. Main wash duration curve fit

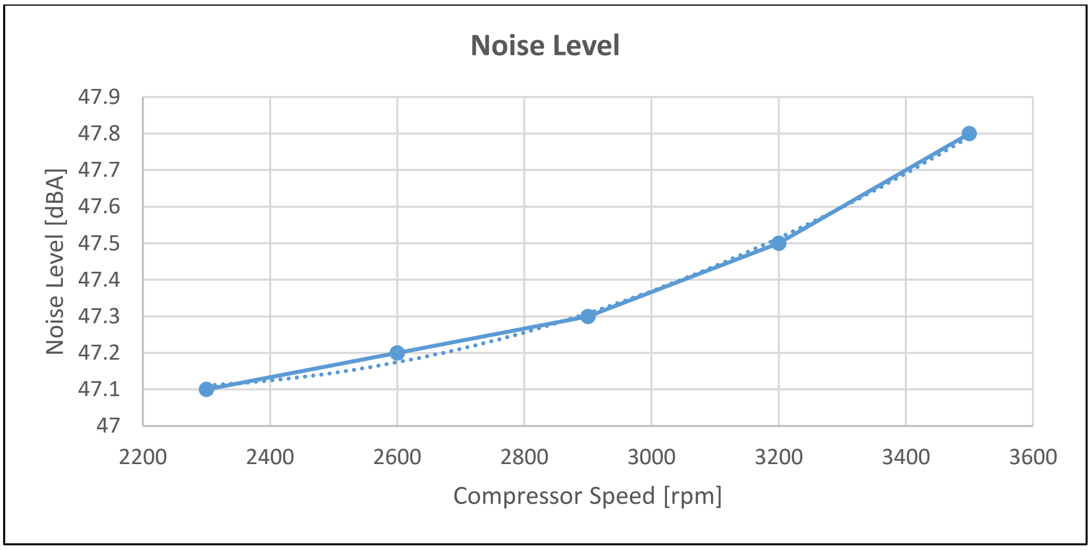

Figure 6.11. Noise level curve fit

Regression analyses have also been conducted for air flow rate as independent variable, and energy consumption, operating time and noise level as dependent variables. The regression lines are shown in Figure 6.12. – 6.14.

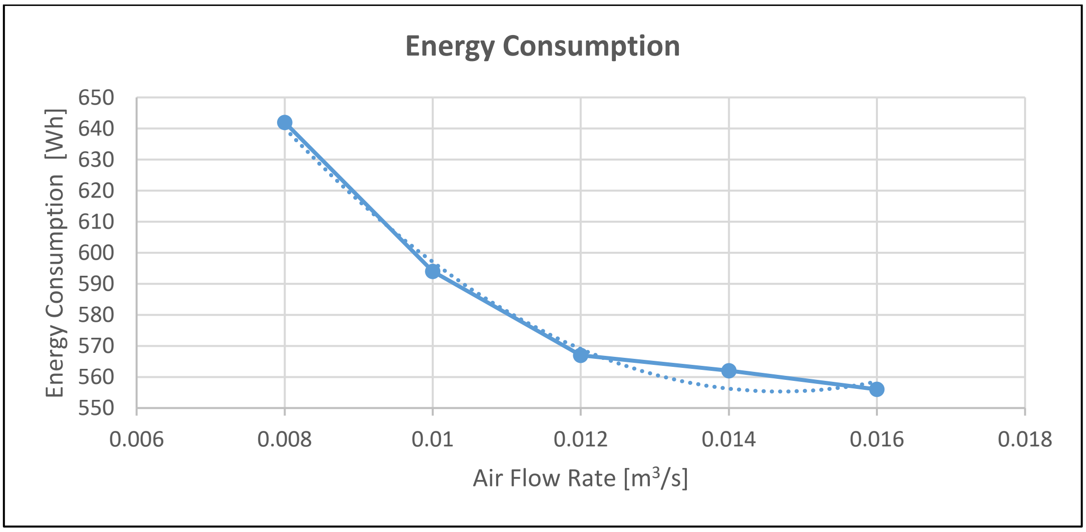

Figure 6.12. Energy consumption curve fit

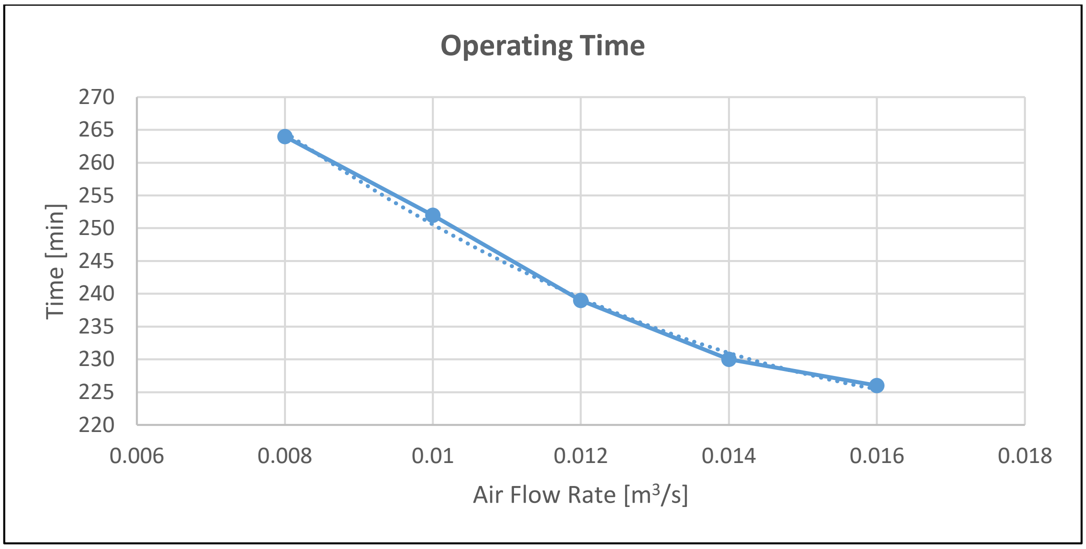

Figure 6.13. Main wash duration curve fit

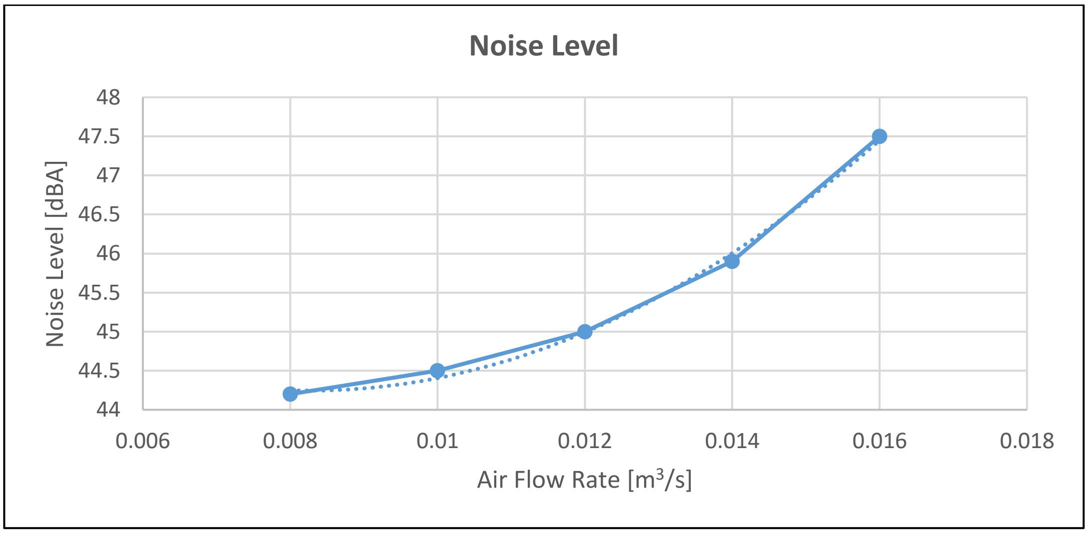

Figure 6.14. Noise level curve fit

Curve fit equations for energy consumption (E), operating time (t) and noise level (A) as a function of compressor speed (N) and air flow rate ($\dot{V}$) is of the form:

$$f(N) = a \times N^3 + b \times N^2 + c \times N + d \qquad (11)$$

or

$$f(\dot{V}) = a \times \dot{V}^3 + b \times \dot{V}^2 + c \times \dot{V} + d \qquad (12)$$

Coefficients of the equations are tabulated in Table 6.13.

Table 6.13. Coefficients of curve fit equations

	a	b	c	d
E (N)	-1.2963E-07	0.001257937	3.957142857	4584.977
t (N)	0	3.33333E-05	-0.242	656.6667
A (N)	0	3.96825E-07	-0.001734921	49.00254
E ($\dot{V}$)	0	1892857.14	-55628.57	964.0286
t ($\dot{V}$)	0	357142.86	-13471.43	349.5714
A ($\dot{V}$)	0	53571.43	-885.7142857	47.90571

According to impact of compressor speed and air flow rate, weighting coefficients are calculated and implemented. Energy consumption, operating time and noise level objective functions are presented in final forms as below:

$$E\ (N, \dot{V}) = 0.25 \times (-0.00000012962963 \times N^3 + 0.001257936507936 \times N^2 - 3.95714285714216 \times N + 4584.97671957609) + 0.75(1892857.14285719 \times \dot{V}^2 - 55628.5714285728 \times \dot{V} + 964.028571428579) \qquad (13)$$

$$t\ (N,\dot{V}) = 0.727 \times (0.000033333333333334 \times N^2 - 0.242000000000005 \times N\ \ + 656.666666666675) + 0.273 \times (\ 357142.857142895 \times \dot{V}^2 - 13471.4285714294 \times \dot{V} + 349.571428571433) \quad (14)$$

$$A\ (N,\dot{V}) = 0.725 \times (0.00000039682539682527 \times N^2 - 0.00173492063492016 \times N\ +\ 49.0025396825393) + 0.275 \times (53571.428571444 \times \dot{V}^2\ -\ 885.71428571467 \times \dot{V}\ +\ \ 47.9057142857164) \quad (15)$$

Since the advantage of heat pump system is energy saving, the most critical objective function is energy consumption. The second critical function is noise level due to acoustic performance of household appliances are affecting costumer comfort significantly. The least critical objective function is operating time. It is also an important parameter however there is not any declaration related to operating time in the energy label in current standard.

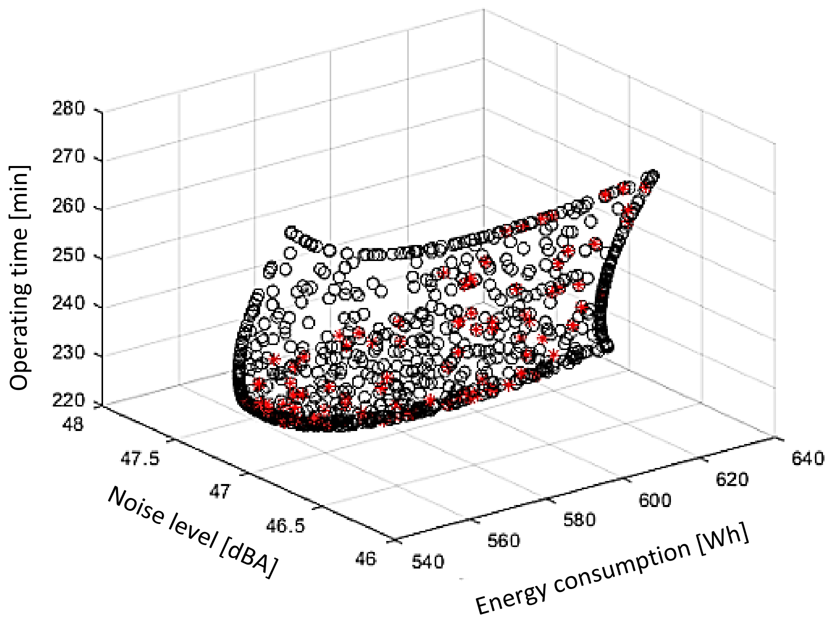

Figure 6.15. Pareto front results

After obtaining pareto front, one suitable parameter combination needs to be selected. The most optimum solution is found by using a rating function which is shown below:

$$Opt_{Result} = C_1 \times \frac{E(N,\dot{V}) - E(N,\dot{V})_{Min}}{E(N,\dot{V})_{Max} - E(N,\dot{V})_{Min}} + C_2 \times \frac{t(N,\dot{V}) - t(N,\dot{V})_{Min}}{t(N,\dot{V})_{Max} - t(N,\dot{V})_{Min}} + C_3 \times \frac{A(N,\dot{V}) - A(N,\dot{V})_{Min}}{A(N,\dot{V})_{Max} - A(N,\dot{V})_{Min}} \quad (16)$$

where;

$$C_1 + C_2 + C_3 = 1 \quad (17)$$

and the coefficients C_1, C_2 and C_3 are related to the importance of the objective functions $E(N, \dot{V})$, $t(N, \dot{V})$, $A(N, \dot{V})$. Since in the present study energy consumption is the most important objective function and the operating time is the least, C_1, C_2 and C_3 are selected as 0.5, 0.2 and 0.3, respectively. These weighting coefficients can be varied depending on the needs in product range. Using optimization results presented in Figure 6.15., rating function is calculated for selected constants. Corresponding parameter values of the optimum point are found to be N= 2800.834 rpm and $\dot{V}$= 0.013074 m^3/s. As a result, objective function results after optimization procedure are, E= 550.6151 Wh, A= 46.7686 dBA and t= 238.7537 min.

In order to validate optimization result, $E(N,V)_{Min}$, $E(N,V)_{Max}$, $t(N,V)_{Min}$, $t(N,V)_{Max}$, $A(N,V)_{Min}$ and $A(N,V)_{Max}$ are calculated with taking derivatives of curve fit equations of Eqn. 13, 14 and 15. Similarly, derivative of Opt_{Result} function is calculated. Minimum of the Opt_{Result} function is found using where the derivative function equals zero. Corresponding parameter values of the optimum point are found to be N=2817 rpm and $\dot{V}$= 0.01315 m^3/s and connected objective function results after optimization procedure are, E= 550.4405 Wh, t= 238.0251 and A= 46.78 dBA min. Sample calculation is given in Appendix B. As seen, the results of MOPSO and derivative are very close. Minor differences are due to rounding errors. As a result, it is shown that MOPSO results are reliable and can be used for optimization.

CHAPTER 7

DISCUSSION AND CONCLUSION

7.1. General

In this thesis study, comparison of ERDW with HPIDW system characteristics have been done. The results state the applicability of heat pump system for a domestic dishwasher in the market.

Nowadays, energy efficiency is an important issue as a result of the increase in consciousness of saving resources and the environment. This thesis study shows that, it is beneficial to integrate heat pump system in the domestic dishwasher in order to decrease energy consumption significantly.

The main advantage and disadvantage of heat pump integration are 302 Wh decrease in energy consumption and increase of noise level, respectively. Noise level increases up to 46.8 dBA due to compressor and fan, yet, it is not causing discomfort since it is similar with refrigerator noise. Heating time is longer with HPIDW system with respect to ERDW. However, cleaning program algorithm is changed in order to eliminate this elongation of heating time.

302 Wh decrease in energy consumption for HPIDW is obtained at the optimum point with modified cold rinse and drying steps. However, it is not the point of minimum energy consumption, since noise level and operating time are also considered in the optimization. Optimum point shows the result of interaction of three objective functions: energy consumption, noise level and operating time.

The integration and component maintenance costs of heat pump system is higher than electric resistance, however, usage fee decreases due to energy efficiency and the HPIDW system pay off its initial cost in time. The comparison of ERDW and optimized HPIDW in terms of energy consumption, noise level and operating time are tabulated in Table 7.1.

Table 7.1. Comparison of ERDW and optimized HPIDW

	ERDW	Optimized HPIDW	Absolute Difference
Energy Consumption (E) [Wh]	853	551	302
Operating Time (t) [min]	235	239	4
Noise Level (A) [dBA]	43.3	46.8	3.5

New regulation for domestic dishwashers will be valid starting from 2021. It is thought that sale of the products below D energy level will be banned with the new regulation. The highest energy class in the market will be A level. The ERDW which has 853 Wh energy consumption is currently classified as A+++ energy level. According to new regulation draft, it will be equivalent to C energy level. The experiment and optimization results show that HPIDW is in A+++-35% energy level considering present regulations and will have at A energy level with new regulations.

In this study, MOPSO is used as optimization tool. It is easy to implement and gives fast solutions. With the help of MATLAB software, MOPSO code is run and objective functions obtained from experiment data are to be minimized considering weights defined for each of them. Since there is no limitation of the number of variables and objective functions, optimization can be improved in future studies. One advantage of MOPSO is that required computation time is lower when comparing to other techniques. Therefore, numerous trial and error runs have been done to achieve best solution in short time.

Energy consumption, operation time and noise level experiments have been done. To prepare experiment setup, prototype of HPIDW is produced. 3D printers are used to manufacture condenser, evaporator and fan casings, connection hoses, compressor insulations and dishwasher chassis. Therefore, experiment setup cost is high. In order to fit the heat pump system into the bottom of dishwasher, current dishwasher components are redesigned due to space limitation and numerous mechanical designs have been done. All the new designs are required to water tight, therefore adhesives are used in assembly. Each time, water resistance is tested to prevent leakage in the energy consumption and noise level experiments.

In order to perform analytical validation, pressure transducers and thermocouples are inserted to the heat pump components and inside of dishwasher tub. Data from these sensors are recorded. Since the components are close to each other, thermocouples are insulated to prevent noise from other heat sources and air flow. Unlike current dishwasher experiments, HPIDW experiments are affected by ambient air and basement conditions highly. Due to this reason, air flow rate inside the test room, basement temperature and distance between test units are controlled also.

7.2. Cost Analyses

Cost analyses have been done in order to determine amortization of heat pump system cost with decrease in energy consumption cost. Domestic A+++ energy level ERDW price is taken as 3009 TL [58]. HPIDW price is assumed 3773 TL considering components costs of heat pump system. Since heat pump components are expensive due to limited production amounts and demand, initial cost is high. However, with increasing HPIDWs' production in years, the initial cost will decrease. For cost analyses, it is assumed that 764 TL initial cost is decreased 5% yearly. In calculations, energy unit cost and inflation rate are considered to be changing with the same trend from 2010 to 2016. Dishwasher price is increasing according to durable consumer goods, electrical and non-electrical appliances consumer price index (CPI) change and energy consumption cost is increased with energy CPI change [59]. In calculations, a dishwasher cycle time is assumed 300 times in a year according to EN50242 [23].

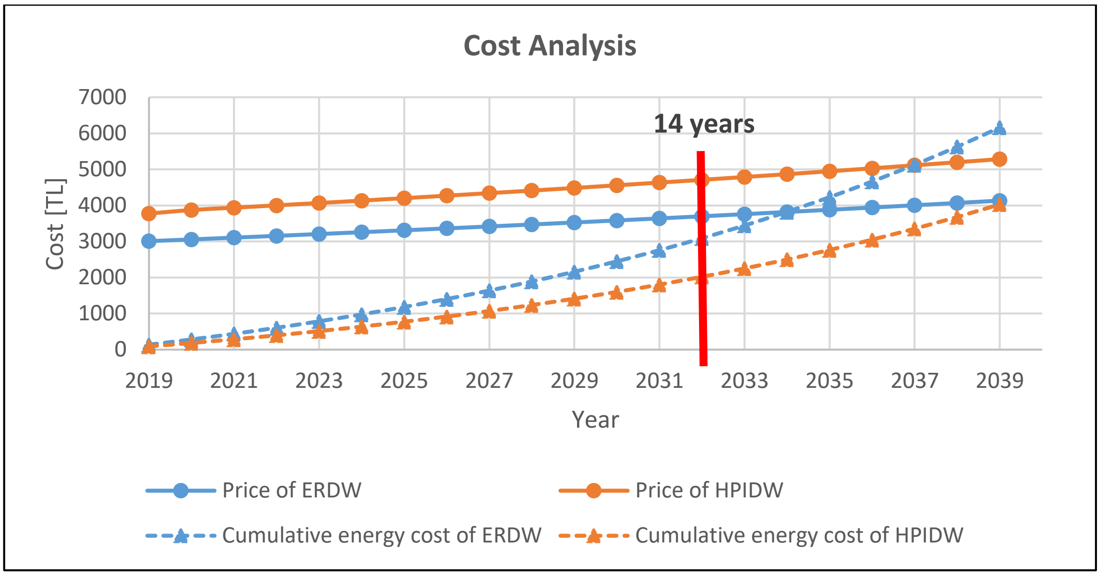

Figure 7.1. Cost Analysis

It is obtained that; heat pump system initial cost is amortized with decrease in energy consumption of HPIDW with respect to ERDW in 14 years as shown in Figure 7.1. After 14 years, cumulative energy cost difference of HPIDW and ERDW is equal to the price difference of HPIDW and ERDW in the market. Since there is a long amortization time, heat pump system seems expensive. However, due to regulation change in the Europe and increasing consciousness about environment protection, it will be obligatory to produce these systems in following years. Heat pump components prices will be lowered when heat pump integrated household appliances become widespread. Improvement in heat pump production technology will also decrease the manufacturing costs in future.

7.3. Recommendations for Future Work

In this thesis study, HPIDW experiments have been conducted and optimized. For optimization, compressor speed and air flow rate are considered as parameters. Components designs (evaporator, fan, compressor and condenser) were not being changed. Since space under dishwasher inner tub is restricted, evaporator and condenser sizes are limited in the experiments. For further studies, undersized components can be designed. Mini-channel evaporator and condenser can improve heat transfer rate and it can be possible to achieve better energy efficiency level.

In the experiments of heat pump system, two fans are used in order to increase heat transfer from air to refrigerant inside of evaporator. One disadvantage of using two fans is increase in noise level. Combination of two equal noise sources are resulting in increase 3 dBA noise level [60]. If same air flow rate is achieved with one fan, single fan can be used, and noise level can be decreased.

Optimization could be adjusted for different energy efficiency level, operating time and noise level. With the help of optimization, different dishwasher performances can be reached, and heat pump system integration may be extended in all dishwasher product range.

In this study, air source heat pump system is integrated to the dishwasher. Advantage of the system is that, heat source is ambient air and it is assumed infinite, therefore dishwasher can be operated continuously. However, water source heat pump system experiments can be made. Fan is not required in this case and noise from fan can be eliminated. Evaporator is inserted into a water thank and heat is transferred from water to the refrigerant inside evaporator. However, since the heat source is water and it is limited, it is necessary to wait until the temperature of water in the tank increased to operable temperature. Though this time, dishwasher cannot be used effectively and in order to heat cleaning water, resistance heater is necessary. Water source heat pump system studies have been done in the literature lately [3].

REFERENCES

[1] L. S. Kokkinides, "Toward Market Transformation: Commercial Heatpump Water Heaters for the ‘‘New York Energy Smarts Region" Final Report," The New York State Energy Research And Development Authority, Albany, NY, 2002.

[2] D. Bosseboeuf, "Energy Efficiency Trends and Policies in the Household and Tertiary Sectors: An Analysis Based on the ODYSSEE and MURE Databases," ADEME-Agence de l’Environnement et la Maitrise de l’Energie, EU, 2015.

[3] P. Bengtsson, J. Berghel and R. Renström, "A Household Dishwasher Heated by a Heat Pump System Using an Energy Storage Unit with Water as the Seat Source," *International Journal of Refrigeration,* pp. 19-27, 2015.

[4] F. Fardoun, I. Oussama and A. Zoughaib, "Quasi-Steady State Modeling of an Air Source Heat Pump Water Heater," *Energy Procedia,* pp. 325-330, 2011.

[5] H. Zhang, S. Shao, H. Xu, H. Zou, M. Tang and C. Tian, "Numerical Investigation on Fin-tube Three-fluid Heat Exchanger for Hybrid Source HVAC&R Systems," *Applied Thermal Engineering,* pp. 157-164, 2016.

[6] T. Mohapatra, N. B. Padhi and S. S. Sahoo, "Experimental Investigation of Convective Heat Transfer in an Inserted Coiled Tube Type Three Fluid Heat Exchanger," *Applied Thermal Engineering,* pp. 297-307, 2017.

[7] P. Bengtsson and T. Eikevik, "Reducing the Global Warming Impact of a Household Heat Pump Dishwasher Using Hydrocarbon Refrigerants," *Applied Thermal Engineering,* pp. 1295-1302, 2016.

[8] P. Bengtsson and J. Berghel, "Concept Study of a New Method for Drying Dishware in a Heat Pump Dishwasher," *Energy Efficiency,* pp. 1529-1538, 2017.

[9] S. Flück, M. Kleingries, E. Dober and B. Wellig, "Dishwasher with Integrated Heat Pump," *HPT Magazine,* pp. 40-44, 2017.

[10] P. Bengtsson and J. Berghel, "Study of Using a Capillary Tube in a Heat Pump Dishwasher with Transient Heating," *International Journal of Refrigeration,* pp. 1-9, 2016.

[11] S. Flück, M. Kleingries, E. Dober, I. Gau, P. Bon, A. Loichinger and B. Wellig, "Household Dishwasher with a Monovalent Heat Pump System," 2017.

[12] A. Abu-Heiba, M. Malhotra, K. R. Gluesenkamp and V. K. Patel, "Domestic Dishwasher Simulated Energy Efficiency Evaluation Using Thermoelectric Heat Pump for Water Heating and Dish Drying," in *5th International High Performance Buildings Conference at Purdue*, Purdue, 2018.

[13] J. Park and A. M. Jacobi, "Energy Efficiency Improvement in a Water Heater With a Run-Around Heat Exchanger System," in *International Refrigeration and Air Conditioning Conference*, Purdue, 2008.

[14] J. Peng, H. Li and C. Zhang, "Performance Comparison of Air-source Heat Pump Water Heater with Different Expansion Devices," *Applied Thermal Engineering,* pp. 1190-1200, 2016.

[15] W. Zhang, X. Huang, X. Gao and H. Yin, "A Constrained Multi-Objective Particle Swarm Optimization Algorithm Based on Adaptive Penalty and Normalized Non-Dominated Sorting," *International Journal of Innovative Computing, Information and Control,* pp. 1835-1853, 2015.

[16] S. S. Hosseini, S. A. Hamidi, M. Mansuri and A. Ghoddosian, "Multi Objective Particle Swarm Optimization (MOPSO) for Size and Shape Optimization of 2D Truss Structures," *Perodica Polytechnica,* pp. 9-14, 2015.

[17] A. Chatterjee and P. Siarry, "Nonlinear Inertia Weight Variation for Dynamic Adaptation in Particle Swarm Optimization," *Computers and Operations Research,* pp. 859-871, 2006.

[18] C. A. C. Coello, G. T. Pulido and M. S. Lechuga, "Handling Multiple Objectives with Particle Swarm Optimization," *IEEE Transactions on Evolutionary Computation*, pp. 256-279, 2004.

[19] C. K. Goh, K. C. Tan, D. S. Liu and S. C. Chiam, "A Competitive and Cooperative Co-evolutionary Approach to Multi-objective Particle Swarm Optimization Algorithm Design," *European Journal of Operational Research,* pp. 42-54, 2010.

[20] Y. Jiang, T. Hu, C. Huang and X. Wu, "An Improved Particle Swarm Optimization Algorithm," *Applied Mathematics and Computation*, pp. 231-239, 2007.

[21] Y. Kao and E. Zahara, "A Hybrid Genetic Algorithm and Particle Swarm Optimization for Multimodal Functions," *Applied Soft Computing,* pp. 849-857, 2008.

[22] S. Lin, K. Ying, S. Chen and Z. Lee, "Particle Swarm Optimization for Parameter Determination and Feature Selection of Support Vector Machines," *Expert Systems with Applications,* pp. 1817-1824, 2008.

[23] EN50242, "Electric Dishwashers for Household Use Methods for Measuring the Performance," *European Standards*, 2008.

[24] IEC-60436:2004, "Electric Dishwashers for Household Use - Methods for Measuring the Performance," *International Electrotechnical Commission International Standard,* 2004.

[25] Y. A. Cengel and M. A. Boles, Thermodynamics an Engineering Approach Fifth Edition, McGraw-Hill, 2006.

[26] TEE, "Technical Data Sheet," Turk Electric Hermetic Compressors, 2018.

[27] Sunon, "Engineering Sample Specifications," Sunonwealth Electric Machine Industry CO., LTD., Taiwan.

[28] United Nations Environment Programme Ozone Secretariat, *The Montreal Protocol,* Montreal: UN, 1987.

[29] United Nations Framework Convention on Climate Change, "The Kyoto Protocol," UN, Kyoto, 1997.

[30] NR, "Safety Data Sheet Refrigerant R134a," National Refrigerants Ltd., USA, 2012.

[31] D. Sanchez, R. Cabello, R. Llopis, I. Arauzo, J. Catalan-Gil and E. Torrella, "Energy Performance Evaluation of R1234yf, R1234ze(E), R600a, R290 and R152a as Low-GWP R134a Alternatives," *International Journal of Refrigeration,* vol. 74, pp. 269-282, 2017.

[32] S. S. Hastak and J. M. Kshirsagar, "Comparative Performance Analysis of R600a and R436a as an Alternative of R134a Refrigerant in a Domestic Refrigerator," *International Conference on Mechanical, Materials and Renewable Energy,* no. 377, 2018.

[33] M. M. Joybari, M. S. Hatamipour, A. Rahimi and F. G. Modarres, "R134a and R600a Energy Efficiency Index Comparison in a Domestic Refrigerator Using Iranian and European Standards," *The 9th International Energy Conference,* 2013.

[34] S. E. Reddy, V. Raju and P. T. Sai, "Comparative Performance Analysis of Domestic Refrigerator Using R12, R134a and R600a Refrigerants," *International Journal of Research and Analytical Reviews,* vol. 5, no. 3, pp. 33-38, 2018.

[35] Keysight Technologies, "34970A Data Acquisition/Switch Unit Family Technical Overview," [Online]. Available: https://literature.cdn.keysight.com/litweb/pdf/5965-5290EN.pdf?id=1000031228:epsg:dow. [Accessed 08 2019].

[36] GW Instek, "GPC-Series Specifications," [Online]. Available: https://www.gwinstek.com/en-GB/products/downloadSeriesSpec/1217. [Accessed August 2019].

[37] MCP Lab Electronics, "SG1634N, SG1638N, SG1640N & SG1642N Product Details," [Online]. Available: http://www.mcpsh.com/pd.jsp?id=124. [Accessed August 2019].

[38] J. Kennedy and R. C. Eberhart, "Particle Swarm Optimization," *IEEE International Conference on Neural Networks*, pp. 1942-1948, 1995.

[39] J. Kennedy, R. C. Eberhart and Y. Shi, Swarm Intelligence, San Francisco: Morgan Kaufmann Publishers, 2001.

[40] K. O. Jones, "Comparison of Genetic Algorithm and Particle Swarm Optimization," *International Conference on Computer Systems and Technologies*, vol. 3, pp. 1-6, 2005.

[41] P. Vikhar, "Evolutionary Algorithms: A Critical Review and Its Future Prospects," *International Conference on Global Trends in Signal Processing, Information Computing and Communication*, pp. 261-265, 2016.

[42] M. Abdelhalim and S. Habib, "Particle Swarm Optimization for HW/SW Partitioning," *InTech Education and Publishing*, 2009.

[43] R. Hassan, B. Cohanim and O. Weck, "A Comparison of Particle Swarm Optimization and the Genetic Algorithm," *American Institute of Aeronautics and Astronautics*, pp. 1-13, 2004.

[44] E. Elbetagi, T. Hegazy and D. Grierson, "Comparison Among Five Evolutionary-based Optimization Algorithms," *Advanced Engineering Informatics*, vol. 19, pp. 43-53, 2005.

[45] International Electrotechnical Commission, "Household and Similar Electrical Appliances – Test Code for the Determination of Airborne Acoustical Noise," *International Standard IEC 60704-2-3: Particular Requirements for Dishwashers*, 2001.

[46] IEC, Application of Uncertainty of Measurement to Conformity Assessment Activities in the Electrotechnical Sector, Switzerland: The International Electrotechnical Commission, 2007.

[47] K. Birch, Estimating Uncertainty in Testing, London: British Measurement and Testing Association, 2003.

[48] REOTEMP Instrument Corporation, "Type T Thermocouple," [Online]. Available: https://www.thermocoupleinfo.com/type-t-thermocouple.htm. [Accessed August 2019].

[49] Vertiv Group Corp., "Vertiv Liebert," [Online]. Available: https://www.vertiv.com/globalassets/products/thermal-management/room-cooling/liebert-lpc_user-manual.pdf. [Accessed August 2019].

[50] Vertiv Group Corp., "Vertiv Liebert," [Online]. Available: https://www.vertiv.com/globalassets/products/critical-power/uninterruptible-power-supplies-ups/liebert-nx-ups-225-600kva-installation-manual_07.pdf. [Accessed August 2019].

[51] Entes Electronics, "MPR5 Series Network Analyzers Technical Specifications," [Online]. Available: http://www.enteselectronics.com/dosyalar/MPR_53_53S_eng_A3918_rev4.pdf. [Accessed August 2019].

[52] IEC, "Household and Similar Electrical Appliances Test Code for Determination of Airborne Acoustical Noise," International Electrotechnical Commission, Switzerland, 2013.

[53] Brüel&Kjær Sound&Vibration Measurement, "System Data," [Online]. Available: https://www.bksv.com/media/doc/bu0228.pdf. [Accessed August 2019].

[54] Brüel&Kjær Sound&Vibration Measurement, "Product Data," [Online]. Available: https://www.bksv.com/media/doc/Bp1380.pdf. [Accessed August 2019].

[55] W. C. Reynolds, "Thermodynamic Properties in SI," Stanford University, Stanford, 1979.

[56] G. Cüylan, "Development of Property Equations for Butane and Isobutane - Preliminary Design of Household Refrigeration Cycle," Department of Mechanical Engineering METU, Ankara, 2009.

[57] Ö. Bayer, "Performance Improvement of Household Refrigerators," Department of Mechanical Engineering METU, Ankara, 2002.

[58] "Arçelik," 2019. [Online]. Available: www.arcelik.com.tr/bulasik-makinesi/6588-i-bulasik-makinesi. [Accessed 28 July 2019].

[59] TCMB, "Enflasyon Raporları," 2019. [Online]. Available: www.tcmb.gov.tr. [Accessed 27 July 2019].

[60] D. Davis and E. Patronis, Sound System Engineering 3rd Edition, USA: Elsevier, 2006.

APPENDICES

A. Sample Calculation of Power Supplied by Compressor

Sample calculation of power supplied by compressor for 3500 rpm compressor speed and 0.016 m^3/s air flow rate in 20^{th} min of operating time.

$$\dot{Q}_{air} = \dot{V} * C_{p,air} * \rho_{air} * \Delta T_{air} \tag{4}$$

$\dot{V} = 0.016\, m^3/s$

$C_{p,air} = 1.006\, kj/kg.K$ (for average air temperature = 10.29 ℃)

$\rho_{air} = 1.25\, kg/m^3$ (for average air temperature = 10.29 ℃)

$\Delta T_{air} = \left(21.77 - (-1.19)\right)$℃

$\dot{Q}_{air} = 0.016 * 1.006 * 1.25 * 22.96$

$\dot{Q}_{air} = 460.56\, W$ (Transferred heat from air to refrigerant in evaporator)

$$\dot{m} = \frac{N * \eta_V * V_P}{\upsilon_1 * 60} \tag{5}$$

$\mathrm{N} = 3500\ \mathrm{rpm}$

$\upsilon_1 = 0.2630\, m^3/kg$

$$\eta_V = (1 + C) * \left(\frac{P_s}{P_l}\right)^{\frac{1}{n}} - C * \left(\frac{P_d}{P_l}\right)^{\frac{1}{m}} - f_{leakage} * \left(\frac{P_d}{P_s}\right) \tag{6}$$

$f_{leakage} = 0.01$

$C = 0.05$

$$P_s = P_l * f_{ps} \tag{7}$$

$P_s = 1.32\, bar$

$$P_d = {P_h}/{f_{pd}} \tag{8}$$

$P_d = 5.38\ bar$

$\eta_V = 0.7634$

$$V_P = \frac{\pi * D^2}{4} * L \tag{9}$$

$D = 25.4 * 10^{-3}\ m$

$L = 22.3 * 10^{-3}\ m$

$V_P = 1.129 * 10^{-5}\ m^3$

$\dot{m} = 1.91\ g/s$

$\dot{Q}_{air} = \dot{m} * (h_1 - h_4)$

$h_1 - h_4 = 240.83\ kj/kg$ (Enthalpy difference between inlet and exit states of evaporator)

$$\dot{W} = \dot{m} * (h_2 - h_1) \tag{10}$$

$h_4 = 270.00\ kj/kg$

$h_1 = 510.83\ kj/kg$

$h_2 = 617.24\ kj/kg$

$\dot{W} = 203.51$ W (Power supplied by compressor at 20^{th} min)

B. Sample Calculation of Optimization Using Derivatives

$$\mathrm{E}\ (\mathrm{N}, \dot{\mathrm{V}}) = 0.25 \times (-0.00000012962963 \times \mathrm{N}^3 + 0.001257936507936 \times \mathrm{N}^2 - 3.95714285714216 \times \mathrm{N} + 4584.97671957609) + 0.75(1892857.14285719 \times \dot{\mathrm{V}}^2 - 55628.5714285728 \times \dot{\mathrm{V}} + 964.028571428579)$$

Derivative of $\mathrm{E}(\mathrm{N}, \dot{\mathrm{V}})$ is obtained;

$$\frac{d\mathrm{E}\ (\mathrm{N}, \dot{\mathrm{V}})}{dN} = -9.72222\mathrm{E}-08 \times N^2 + 0.000628968 \times N - 0.989285714$$

$$0 = -9.72222\mathrm{E}-08 \times N^2 + 0.000628968 \times N - 0.989285714$$

$N = 2698.3$ (this is where $\mathrm{E}(\mathrm{N}, \dot{\mathrm{V}})$ is minimum for N. The other N value is 3771.1 where is located outside of defined boundary and gives max value.)

$$\frac{d\mathrm{E}\ (\mathrm{N}, \dot{\mathrm{V}})}{d\dot{\mathrm{V}}} = 2839285.714 \times \dot{\mathrm{V}} - 41721.429$$

$$0 = 2839285.714 \times \dot{\mathrm{V}} - 41721.429$$

$\dot{\mathrm{V}} = 0.0147$ (this is where $\mathrm{E}(\mathrm{N}, \dot{\mathrm{V}})$ is minimum for $\dot{\mathrm{V}}$.)

$E_{min} = 546.3739$ ($\mathrm{E}(\mathrm{N}, \dot{\mathrm{V}})$ function is solved for obtained N and $\dot{\mathrm{V}}$ values.)

Below max and min values are obtained using Figure 6.9 – 6.14.

$E_{max} = 626.8142$ (max point is the boundary limit at N=3500 rpm and $\dot{\mathrm{V}}$=0.008 m^3/s)

$t_{min} = 220.0358$ (min point is the boundary limit at N=3500 rpm and $\dot{\mathrm{V}}$=0.016 m^3/s)

$t_{max} = 273.1942$ (max point is the boundary limit at N=2300 rpm and $\dot{\mathrm{V}}$=0.008 m^3/s)

$A_{min} = 46.3241$ (max point is the boundary limit at N=3500 rpm and $\dot{\mathrm{V}}$=0.016 m^3/s)

A_{max} = 47.6971 (max point is the boundary limit at N=2300 rpm and $\dot{V}$=0.008 m^3/s)

Below constants are already defined according to the importance of objective functions.

$C_1 = 0.5$
$C_2 = 0.2$
$C_3 = 0.3$

All defined and determined values are inserted to the equation and derivative is obtained.

$$Opt_{Result} = C_1 \times \frac{E(N,\dot{V}) - E(N,\dot{V})_{Min}}{E(N,\dot{V})_{Max} - E(N,\dot{V})_{Min}} + C_2 \times \frac{t(N,\dot{V}) - t(N,\dot{V})_{Min}}{t(N,\dot{V})_{Max} - t(N,\dot{V})_{Min}} + C_3 \times \frac{\mathrm{A}(\mathrm{N},\dot{\mathrm{V}}) - \mathrm{A}(\mathrm{N},\dot{\mathrm{V}})_{\mathrm{Min}}}{\mathrm{A}(\mathrm{N},\dot{\mathrm{V}})_{\mathrm{Max}} - \mathrm{A}(\mathrm{N},\dot{\mathrm{V}})_{\mathrm{Min}}}$$

$$\frac{d\mathrm{Opt}_{\mathrm{Result}}}{dN} = -(6.04313E-10 \times N^2) + (4.2176E-06 \times N) - 0.007085945$$

$$0 = -(6.04313E-10 \times N^2) + (4.2176E-06 \times N) - 0.007085945$$

$N = 2817$ (this is where $\mathrm{Opt}_{\mathrm{Result}}$ is minimum for N. The other N value is 4163 where is located outside of defined boundary and gives max value.)

$$\frac{d\mathrm{Opt}_{\mathrm{Result}}}{d\dot{\mathrm{V}}} = 24819.98528 \times \dot{V} - 326.3885114$$

$$0 = 24819.98528 \times \dot{V} - 326.3885114$$

$\dot{\mathrm{V}} = 0.01315$

When E $(\mathrm{N}, \dot{\mathrm{V}})$, t $\left(\mathrm{N}, \dot{\mathrm{V}}\right)$ and A $(\mathrm{N}, \dot{\mathrm{V}})$ are solved with $N = 2817$ and $\dot{\mathrm{V}} = 0.01315$ values optimization result is obtained;

E = 550.4405

t = 238.0251

A = 46.7852